INFLUENCE OF POLARITIES ON EROSION RATES OF COPPER/STEEL ELECTRODES IN EDM PROCESS

by

RANJIT SAHA

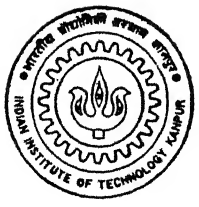

DEPARTMENT OF MECHANICAL ENGINEERING

INDIAN INSTITUTE OF TECHNOLOGY KANPUR

JUNE, 1999

INFLUENCE OF POLARITIES ON EROSION RATES OF COPPER/STEEL ELECTRODES IN EDM PROCESS

A Thesis Submitted

in Partial Fulfilment of the Requirements

for the Degree of

MASTER OF TECHNOLOGY

by

RANJIT SAHA

to the

DEPARTMENT OF MECHANICAL ENGINEERING

INDIAN INSTITUTE OF TECHNOLOGY, KANPUR

June, 1999

CERTIFICATE

It is certified that the work contained in the thesis entitled "**Influence of Polarities on Erosion rates of Copper/Steel electrodes in EDM process**", by Ranjit Saha , has been carried out under my supervision and that this work has not been submitted elsewhere for a degree.

Dr. M.K.Muju
Professor
Department of Mechanical Engineering
I.I.T., Kanpur

June, 1999.

Acknowledgement

I wish to place on record my deep sense of gratitude and indebtedness to Dr. M.K.Muju for his skillful guidance, constant supervision, constructive criticism and encouragement during the course of my thesis work.

Sincere thanks are due to R.M.Jha, H.P.Sharma, Namdeo and Anil for their active support during the course of the experiments carried out in the Manufacturing Science lab. Special thanks to Pabitrada and Raju for the help extended in the latex settings. Finally I would like to thank all my friends and faculty of Manufacturing Science stream for providing me a cordial and pleasant atmosphere and making my stay at IIT Kanpur memorable.

(Ranjit Saha)

June, 1999

Kanpur

Contents

List of Figures

List of Tables

Abstract

In the present work, Electric Discharge machining process has been investigated to study the effects of electrode materials and polarities on the material removal rate. The pointed heat source model (PHSM) for cathode erosion has been evaluated by the experimental results for four sets of electrode pair i.e., MS(-ve)/MS(+ve), Cu(-ve)/Cu(+ve), MS(-ve)/Cu(+ve) and Cu(-ve)/MS(+ve) systems. It has been suggested that the PHSM can be used to estimate the erosion rate from the cathode material with a fair degree of accuracy provided it is assumed that the fraction of energy going to the cathode is a function of energy input per pulse into the system. Some logical justification is given for the above assumption. The material removal rate of cathode is more than the anode in MS(-ve)/MS(+ve),Cu(-ve)/Cu(+ve) and MS(-ve)/Cu(+ve) systems. But in Cu(-ve)/MS(+ve) system the erosion rate of anode is more than that of the cathode. Few of the experimental results have been found comparable to the results of other researchers. It has been observed that Cu anode always results in higher amount of material removal rate from cathode (MS or Cu) compared to MS as anode. It is found that, greater fraction of input energy gets distributed to the electrodes in Cu(-ve)/Cu(+ve) system when compared to MS(-ve)/MS(+ve) system . The sum of erosion rates from the electrodes in MS(-ve)/Cu(+ve) system is significantly greater than that in the Cu(-ve)/MS(+ve) system, thus establishing a special place for copper anode, as compared to steel. Finally, it has been concluded that the distribution of energy per pulse to the electrodes and dielectric, and hence the erosion rates, depends significantly on the electrode material pair as well as the polarity of the electrodes.

Nomenclature

A, B : Constants for the wear ratio

a, b, c : Constants in the average discharge current equation

$C.E$: Cohesive energy

C_p : Specific heat (J/Kg^oK)

E : Total energy input at the interelectrode gap (J)

f : fraction of power lost to an electrode

I : Average discharge current (amp)

K_T : Thermal conductivity (W/m^oK)

q_o : Heat flux (W/m^2)

r : radius of melt front

R : Radius of crater at melting temperature (m)

T : Temperature (^oK)

t : time (sec)

U : Discharge voltage $(Volts)$

V_c : Crater volume (mm^3)

$\dot{V}_w$: Erosion rate (mm^3/min)

Greek symbols

α : Thermal diffusivity (m^2/sec)

ρ : Density (Kg/m^3)

Subscripts

a : anode

c : cathode

d : dielectric

e : electrode

m : melting

o : ambient

off : pulse off

on : pulse on

r : radiation

w : workpiece

Superscript

$'$: MS(−ve)/Cu(+ve) system

$''$: Cu(−ve)/MS(+ve) system

Chapter 1

INTRODUCTION

1.1 Introduction

Electric discharge machining (EDM), also called as Electric spark machining, occurs when a succesion of discrete spark discharges between an electrode and a work material results in preferential erosion of the work-material. To achieve an effective material removal in a controlled manner presence of a suitable dielectric fluid between electrode and the work-material and a direct current power source are important elements of the process. Kerosene is a very common dielectric fluid used. Thermal energy available in discharge pulses is the basis that causes the material removal. When discharge occurs the intense heat generated melts and evaporates the material of the two electrodes and also some debris that have become available in the sparking gap.

Fig.1.1 shows the basic scheme of the process. In resistance and capacitance type of ciucuit an applied voltage of about 200 $Volts$ across a typical gap of 20 to 40 μm causes the dielectric to breakdown. The voltage falls to about 25 $Volts$ after the breakdown. The required discharge conditions can be stabilized by using the servo-controlled feed of the tool electrode to maintain a small working gap. In this situation the forming electrode(tool) reproduces its comlimentary shape

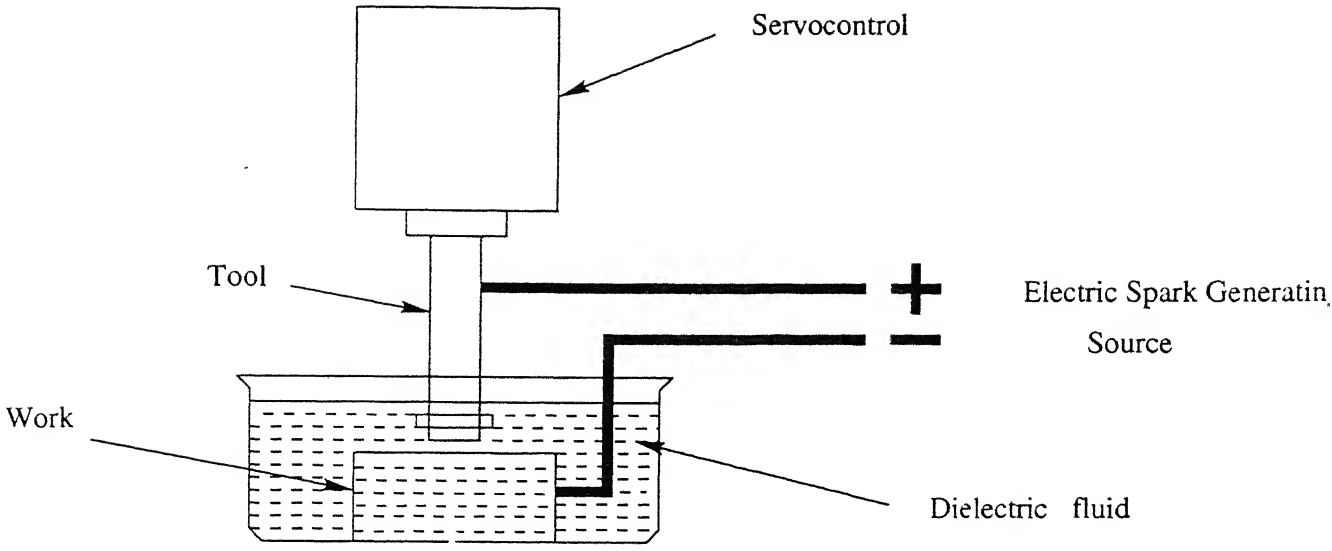

Figure 1.1: Basic scheme of electrical discharge machining

upon the workpiece. It is observed that polarity determines the rate of material removal. When the pulse duration is very small, typically less than 1 micron, the positive electrode erodes faster than the negative electrode. But for larger pulse duration's it is the nagative electrode which erodes faster. And this is true even for similar materials with few exceptions. For this reason in die-sinking machines the work is connected to the negative electrode while in wire EDM machines the wire is connected to the negative terminal of the d.c. supply. This aspect of polarity is discussed later.

As discharge occurs preferentially at the closest locations between the two surfaces, the sparks wander in a random manner all over the surface. This results in uniform material removal over the entire surface and gradually producing a replica of the tool surface into the work-surface. Obviously, only electrically conductive materials can be machined. The process is of great utility in machining very hard and tough metals and alloys including ceramics. Although both the electrodes get eroded, the process conditions are usually adjusted in such a manner as to limit in wear of tool electrode to about one percent or less of the

work-piece erosion.

1.1.1 Pulse Generation

The type of pulse generation system selected for EDM purpose would essentially depend upon the application.

(i) Low energy range (per spark) systems are selected when the objective is to remove small amounts of material as in finishing operations.

(ii) For medium and rough machining purpose, controlled pulse generators are used. In these systems the pulse duration, pulse profile and repetition time can be controlled and suitably selected.

(i) Low energy range systems Resistance-capacitance relaxation circuits with a constant d.c. source represent this class. Supply voltages used range from 100 to 500 *Volts* and peak currents are upto 1000 *amps*. Energy supplied to the gap between electrodes is determined by the breakdown voltage (V) and the capacitance (C).

The pulse form and pulse time depend upon the impedance of the discharge circuit, including capacitor and there is little control that can be exercised. In these systems the charge cycle is long compared to discharge time which results in low time utilization of the cycle, hence low efficiency. Also, the reverse half wave can lead to increased tool wear. Since material removal rate with these circuits is low, these systems have preferential use in finishing applications.

(ii) High energy rate systems: In controlled pulse generators, pulse duration and repetition time can be selected and controlled independent of spark conditions leading to more efficient time utilization. The characteristics typical pulse generator circuit is shown in Fig.1.2. Also Fig.1.3 shows the types of pulses obtained in EDM using these machines.

In these generators energy from a d.c. source (60 - 120 V) is supplied to the working gap via a resistor and electronic switch. The magnitude of current level

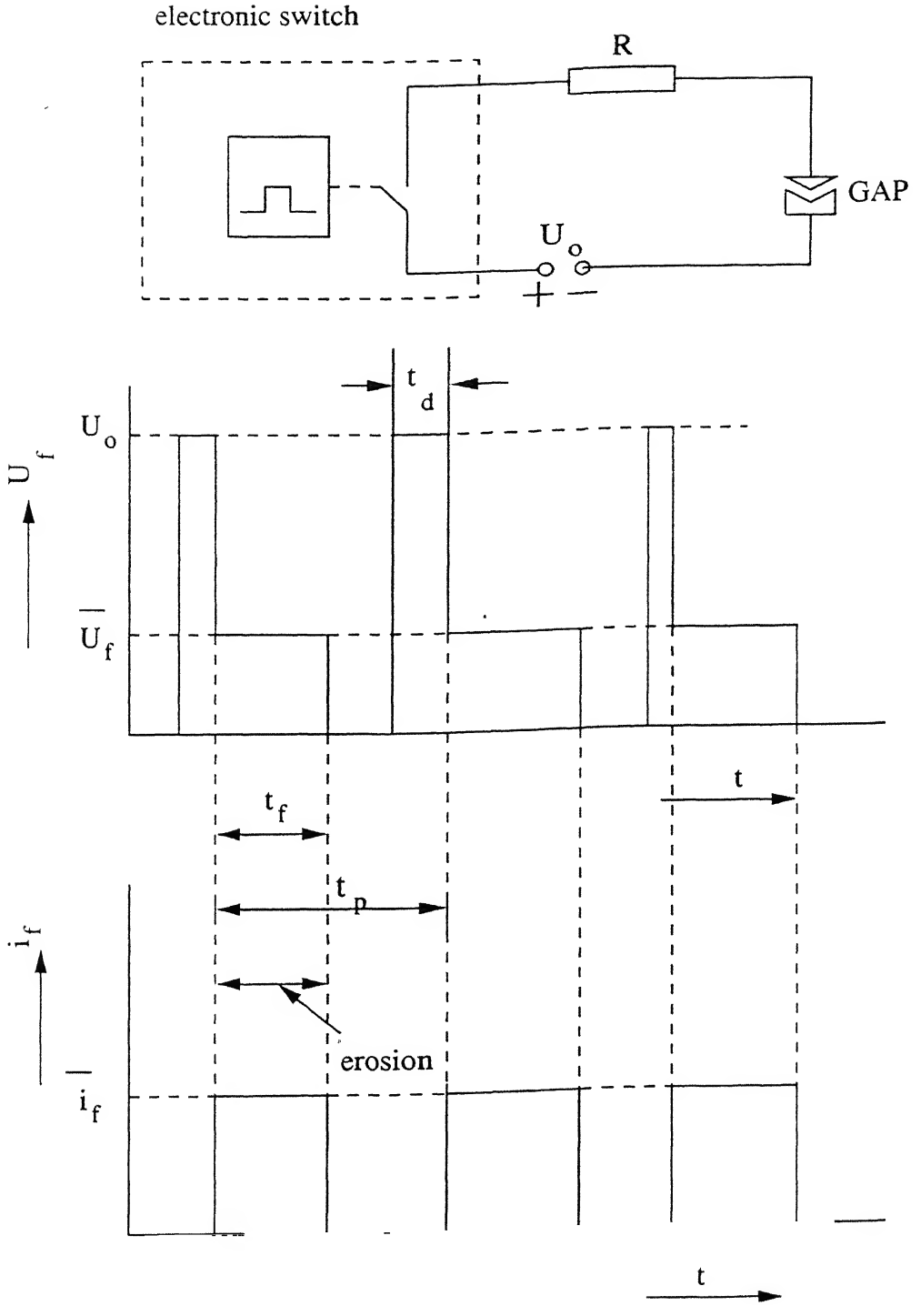

Figure 1.2: Characteristics of a typical pulse generator

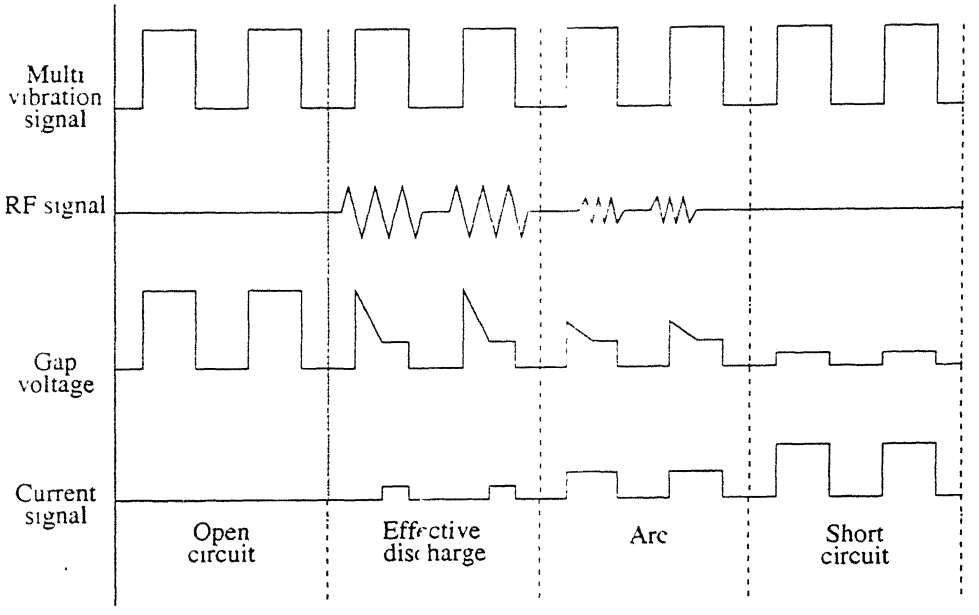

Figure 1.3: Types of pulses in EDM

is determined by the power supply voltage, arc voltage and the resistor. Currents range from 1 *amp* to 100 *amp*. Pulse times obtainable are in the range of 0.1 microsec to several millisecs. The pulse shape is usually rectangular. The relative tool wear is kept low by utilizing suitable pulse time-pulse current ratios. A non-rectangular pulse like a trapezoidal one results in very low relative tool wear. Controlled pulse circuits provide an important feature of automatic stoppage of current flow when a short circuit occurs. Discharge pulses produced by generators as against those from relaxation circuits are unidirectional and hence do not have the disadvantage of reverse material removal. Thus, tool wear is inherently less. This leads to improved reproduction accuracy and higher material removal rates.

1.1.2 Spark Frequency

While an arc is a stable thermionic phenomenon, a spark is a sudden transient and noisy discharge between two electrodes. The latter situation occurs in EDM process. Discharge of approximately 1 micro-second to 1 milli-second are encour-

ages in EDM process. Shorter duration sparks have less energy and consequently remove less material and give better surface finish. However, if the ratio of pulse duration (t_{on}), also called as on-time, to pulse cycle time (t_c) is increased, probablity of arcing is seen to increase, especially for low values of pulse duration. Hence, to avoid arcing, pulse cycle time should be increased. What this implies is that sufficient time needs to elapse before the dielectric quenches the spark and is ready for the next spark. Arcing can also be avoided by periodically widening the working gap to facilitate flushing.

1.1.3 Change from sparking to arcing

Sparking is the ideal machining condition as it gives controlled erosion of workpiece. It is a condition in which several successive sparks are formed each time a voltage pulse is successfully discharged across a gap. These sparks occur in rapid succession and in randomly changing positions resulting in fairly uniform material removal.

Arcing on the other hand is one heavy discharge of energy lasting for most of the pulse time. This is concentrated in one place to give uncontrolled erosion which can severely damage workpiece and electrode. With arcing it is impossible to get good surface finish. Trapezoidal pulse waveform is found to be more efficient than rectangular. However, the latter being easier to produce are more commonly employed. A trapezoidal pulse in which the current is large at the begining and declines linearly produces a crater volume for a single spark that is almost three times that obtained with the standard rectangular pulse. Conversly, using a pulse with higher current towards the end, machining rate is lower while electrode wear is also lower and surface finish is better. Therefore design of an optimum pulse profile is of research and application interest.

1.1.4 Ignition Process

In a typical EDM operation discharge occurs across a narrow gap between the two electrodes when a field strength of about 10,000 V/mm to 100,000 V/mm is established. Discharge, however, occurs only some time after the supply voltage is impressed across the electrodes. This delay is referred to as ignition-delay and can last several micro-seconds. Electrons leaving the cathode by field emission and traveling towards anode result in heating of the fluid available in the gap. After the ignition delay there is local evaporation of the fluid. This produces gas bubbles within which breakdown occurs. When gas bubbles are available, collisional ionisation is also possible, which reduces the resistance of the local current path resulting in considerable increase in field strength. This will increase the dissipated energy and the temperature at the cathode surface increases. This results in transition from field emission to thermal emission which causes an increase in current density upto about 10,000 A/mm^2.

Low boiling point and low specific heat of dielectric fluid like kerosene, facilitates its evaporation and hence the ignition process. Presence of impurities in the working gap cause an increase in the field strength thereby facilitating the field emission. It is estimated that for a current density of 10,000 A/mm^2, the field strength near the cathode is about a million V/mm. Since the voltage drop across the gap is about 20 V, the region of this order of voltage drop has to be very small (5 nm). Such a small magnitude implies that the heat source are virtually acting on the surface of electrodes.

Electric field between the electrodes tends to increase when the voltage across them is increased and gap is decreased. When the field reaches a certain level, electrons get emitted from the cathode. The emitted electrons, together with any available in the gap, are accelerated by the applied field ionizing the neutral particles in their path. The newly generated electrons and ions also get acceler-

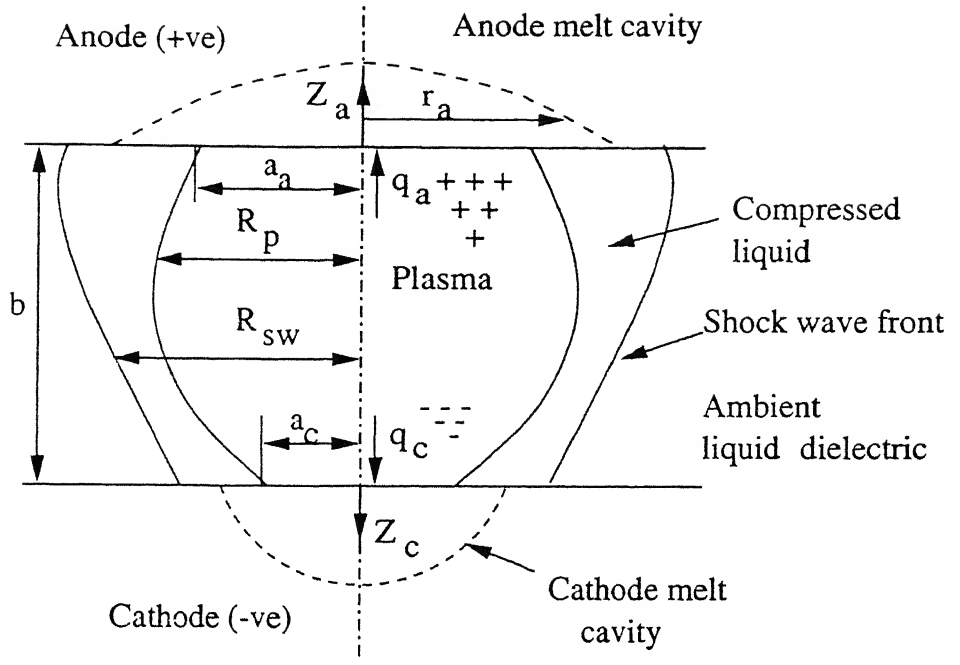

Figure 1.4: A schematic diagram of the EDM process showing the circular heat source, plasma configuration, and melt cavities after a certain on-time

ated towards the anode and cathode respectively causing further ionisation and a chain reaction occurs producing an avalanche of ions. The region in which this avalanche occurs is called plasma channel. Fig.1.4 is a schematic diagram showing the plasma region.

Conditions are then right for a spark to be initiated between the electrode and work. Some atoms and ions are excited by collision leading to emission of light. Part of this light is used in the photo-ionisation of neutral particles, the rest enable the spark to be seen. It takes about 10 ns to 20 ns for the full development of the spark. After the spark is initiated, it can be maintained at a much lower voltage. Most of the voltage drop occurs between the electrodes and the channel and negligible drop occurs across the channel.

Due to the complex activities in the plasma channel, a very high temperature, between 8000-12000 ^{o}C, is reached rapidly causing instantaneous melting of the

electrode and work-material. As the temperature continues to rise, a gas bubble of increased pressure is formed. At the end of the pulse when electricity is cut-off the bubble explodes to create dynamic forces which eject the molten metal from the eroded crater. A percentage of the metal is carried away in the dielectric fluid which is continuously flushed through the gap. The remainder settles on the surface of the crater.

1.1.5 The Plasma region

The situation in the plasma channel is complex, with fast moving electrons, ions and neutral particles all interacting under electrostatic forces and collision. Some atoms and ions excited by collision leading to emission of light. Part of this light is used in the photo-ionisation of neutral particles. The rest enable the spark to be seen. In a dielectric fluid only an extremely short time (10 ns to 20 ns) are adequate for full development of the spark. After the spark is initiated it can be maintained at much lower voltage. Most of the voltage drop occurs between the electrodes and the channel and negligible drop occurs across the channel.

1.1.6 Mechanism of EDM process

A plasma channel, surrounded by a vapor bubble grows during the on-time is usually less than 100 micro-secs. The surrounding dense liquid dielectric restricts the plasma growth. Input energy (UIt_{on}) is thus concentrated in a very small volume. The local plasma temperature as high as 40,000 ^oK are reached. Dynamic plasma pressure rises to as high as 3 $kbar$ due mainly to inertia (density) effects. Viscosity effects are thought to be responsible for the plasma shape of Fig.1.4

The following features of EDM process have been visualized:

i) During the pulse on-time the high energy plasma melts both electrodes by conduction, but limited electrode vaporization occurs due to high plasma pressure.

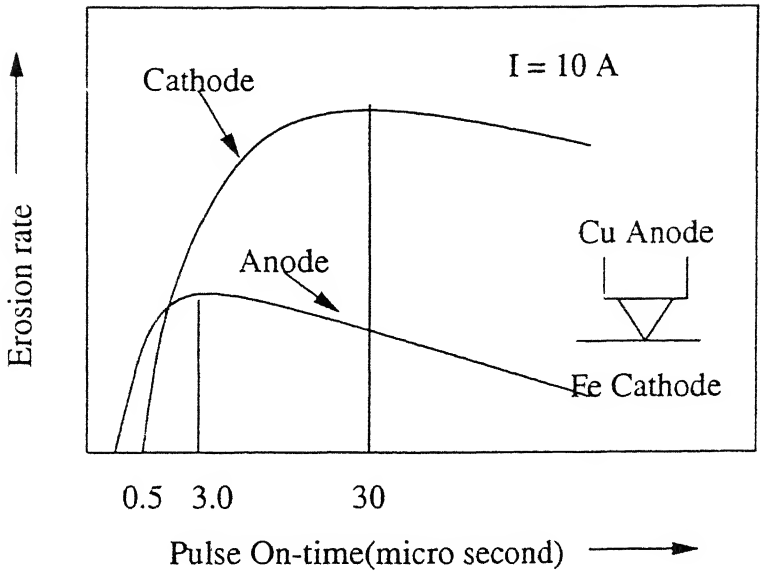

Figure 1.5: The difference between anode and cathode erosion rates with different On-times (not to scale)

ii) Anode first melts rapidly due to absorption of fast moving electrons at the start of the pulse, but then begins to resolidify after a few microseconds. This is thought to be due to expansion of plasma radius at the anode resulting in decrease in local heat flux at anode surface.

iii) Melting of cathode is delayed in time by one or two orders of magnitude beyond that of the anode due to lower mobility of positive ions.

iv) Since cathode is emitting electrons the plasma radius at the cathode is also much smaller, thereby approximating a point heat source for conduction into its interior.

v) The current density decreases strongly with increasing depth beneath the electrode surface. Hence the temperature rise in the electrodes due to Joule heating is found to be negligible.

vi) At the end of on-time (t_{on}), pause time (t_{off}) begins when power is terminated to the machine. During this time a violent collapse of the plasma channel and vapor bubble occurs, causing the super-heated, molten liquid on the surface of

both the electrodes to explode into the liquid dielectric. This leaves cavities of usually less than 100 μm in width on the electrodes thus leaving an ultra-smooth finish.

vii) Fig.1.5 shows how the erosion rate curves for cathode and anode cross over at about 0.5 μsec for a particular case.

viii) For die-sinkers the cathode is usually the workpiece and anode the shaping tool. The optimum pulse times of 10 to 100 $\mu secs$ are used.

ix) For such long on-times, anode erosion is low due to resolidification.

1.2 Literature Review

Several authors have considered the physical events during EDM process and provided explanations to the discharge and erosion phenomenon [1-8]. Mathematical modeling of the process is generally done on the basis of isolated single sparks [6,9-16]. However successive discharges have significant effect on the machining performance [3-6]. It would be very difficult, if not impossible, to consider their effect on the physics of single sparks. Extension of the physics of single sparks to the engineering applications i.e., multiple sparks, can be achieved by an appropriate statistical analysis of pulse trains [4].

Heuvelman et al. [9] have conclusively shown that the breakdown mechanism in EDM is not caused by the collisional ionisation of the liquid molecules as the mean free path in liquids is comparitively small. They have also shown that the ignition delay strongly depends on the energy per unit volume added to the gap, which implies that the ignition delay is strongly dependent on the gap width. They thus propose that it would be better to use ignition delay as a sensor for the servo-system instead of the voltage drop across the electrodes. Eubank et al. [16] have provided a quantitative proof that super-heating is the mechanism responsible for erosion in EDM. Snoeys et al. [17] have shown that

there exist a fairly good correlation between the sum of the discharge durations per sec and the material removal rate indicating that a measurement of the total effective discharge duration could be a reliable in-process measurement of the material removal rate.

Vaseekaran et al. [8] have studied the spark erosion in TiB_2 and Zn on the basis of the effects of the tool electrode geometry, input energy and electrode polarity. Guerrero-Alvarez et al. [3] have studied the electro erosion phenomenon of Fe and Zn by SEM analysis. Cathode craters were always found to be larger than anode craters irrespective of the discharge energy or the electrode material. Cross-deposition from cathode to anode in all samples was larger than the cross-deposition from anode to cathode, independent of energy and material. However, higher concentration of cross-deposited metal is found at the rim of the crater than in the central region due to radial pressure gradient of the discharge column.

Longfellow et al. [18] have studied the behaviour of electrode material properties on the wear ratio experimentally. They have postulated that the intrinsic physical properties of the electrode material that govern the wear ratio are

(i) a combination of thermodynamic constants, which may be summed up in the single term, cohesive energy.

(ii) Mechanical strength and toughness.

(iii) Ratio of evaporation temperature (in ^oK) to melting temperature and

(iv) Electrical resistivity.

The electrode of low resistivity would absorb less thermal energy from resistance heating than one of high resistivity, thereby making available additional energy for heat generation and subsequent erosion of material from the workpiece.

They have given the ralation for wear ratio (W.R.) as

$$W.R(\text{anode erosion rate/ cathode erosion rate}) = A \left[\frac{C.E(\text{cathode})}{C.E(\text{anode})}\right]^B$$

where $C.E$ is the cohesive energy of the material in $kcal/mole$ and A and B

Anode	A	B
Zn	1.85	31.2
Cu	0.39	81.1
Fe	0.40	99.5
Mo	1.55	157.5

Table 1.1: Constants for wear ratio as reported by Longfellow et al. [18]

are constants for a particular workpiece (anode) whose values are given for a few anode materials in Table 1.1. These constants have been obtained for few specific anode (work) material and tool materials (cathode) using regression analysis. The utility is of limited application.

Few experimental observations in the present work also conformed to this relation [Sec2.3.1].

At low pulse times it has been postulated that electrical forces are responsible for the material removal [6-8]. However studies at high pulse times shows that thermal properties are more effective than mechanical properties in the EDM process , and the predominent thermal phenomenon is voporization, rather than melting [3,6-8,18]. Depending on the discharge condition and the material, material equivalent to 10-15% of the final crater volume vaporizes [2,7]. The molten material cannot be removed completely because of surface tension, tensile strength and bonding force between the liquid and solid phase [7,8].

Guerrero-Alvarez et al. [3] have observed a decrease in removal efficiency at higher energy. This is explained on the basis of electrode gap spacing which increases at higher energies in order to maintain the breakdown field constant. As the length of the discharge column is increased , the amount of heat loss, the radial diffusion of ions, and recombination occurring between the anode and cathode drop region also increases. Hence the removal efficiency decreases at higher energies.

George et al. [5] and Albinski [19] have suggested that in order to increase the work erosion rate, the polarity of the electrodes has to be determined experimentally, which depends on tool material, work-material, area and pulse length combination. Heng et al. [20] have proposed a new kind of pulse waveform, known as the polarity-change pulse. The workpiece polarity was changed from positive to negative without allowing plasma extinction during the discharge. He observed greater work-piece removal rate and smaller tool erosion ratio. Erden et al. [2] have indicated that for different pulse durations, there may be different optimum pulse shapes.

Many authors [5,7,8] have studied the effect of debris concentration on erosion and electrode wear. Vaseekaran et al. [8] have reported that the debris tend to move into the discharge channel under the influence of electric field in the gap, leading to rapid fluctuation in the resistance. Erden [7] has observed that addition of metal powders like Al, Cu and Fe in Kerosene dielectric liquid increases erosion rate of both tool and workpiece. However carbon usually results in decrease in the erosion rate. George et al. [5] have observed a higher amount of tool(anode) wear with clean dielectric compared to unfiltered and contaminated liquid.

Study of the effect of dielectric composition on the machining rate [21] has shown that, in general with other conditions being equal, the lowest material removal rate is obtained with oils. It has also been observed that a high efficiency is achieved with Kerosene and it is increased even more with light alcohols and some derivatives of benzene. Thermal capacity of the dielectric fluid is responsible to alter the proportion of heat transmitted through the electrode and hence influence the erosion and erosion ratio of the electrodes.

George et al. [22] have observed a reduction in machining rate with the use of dielectric flushing. However Snoeys et al. [17] have observed almost no effect of dielectric flushing on material removal rate. Konig et al. [6] have reported that

the energy stored in a dielectric fluid follows a curve similar to the sum of erosion and wear rates. Erden et al. [23] have examined and compared eight different thermo-mathematical models for electrode erosion by different reserchers.

Some researchers have studied the energy distribution at the electrodes. It has been reported that the fraction of power going to the cathode depends on the pulse shape, current, pulse duration and type of machining i.e., rough or fine [2.6,7]. Erden [7] has reported that the fraction of power going to the cathode depends on the work function of the material and to some extent on its atomic weight. However DiBitonto et al. [14,15] have considered that the fraction of power going to an electrode is nearly constant for a particular electrode in a particular dielectric liquid and is independent of current and pulse time.

1.2.1 Present state of theoretical models for estimation of erosion rates

A host of researchers have attempted to model the EDM process to estimate the erosion rates and were successful at varying degrees. Some of these are discussed below.

Van Dijck et al. [10] obtained the crater volume in EDM by numerically solving a thermal model. The computational procedure was based on the exact solution of the related two-dimensional transient heat conduction problem in a finite or semi-infinite body subjected to a stepwise or time-dependent uniform heat flux over a small circular part of its upper surface. It is shown that *the theoretical model should include the possibility of accounting for the plasma channel widening* in-order to obtain acceptable agreement with experimental data or to predict the optimal operating conditions.

Pandit et al. [11] modeled EDM process from surface roughness profiles by using data dependent system approach. This method bridges the gap between single discharge approach and the time-averaged approach by defining and ob-

taining a "characteristic crater" from EDMed surface profiles. The characteristics crater accounts for the randomness of the process and includes the effect of mutual interactions and successive dependencies within a train of discharges in the practical domain of electric-discharge machining.

McGeough et al. [12] developed a macroscopic model based upon the assumption that the time dependent electric field can be replaced by an electrostatic field, and the experimental observation that the dielectric breakdown process would start only if the electric field is more than a critical value. They also assumed that the material removal from the tool and work-piece is proportional to the energy transmitted by the spark. The overall shapes of the tool and the work-piece were determined by solving the Laplace equation of electric potential.

Later Pandey et al. [13] have calculated the crater volume by modifying the two-dimensional disk heat source model by accounting for the *growth of the plasma channel during the pulse On-period.* This consideration has led to a marked improvement in the results and correspondence between the theoretical and experimental data. The analytical results also demonstrate the effect of electrode material on the rate of plasma channel growth. This model also enables one to obtain the thickness of heat-affected zone and the extent of thermal damage suffered by the electrode material due to a single spark with a fair degree of accuracy.

A detailed modeling was adopted by DiBitonto et al. [14,15] to find out the material removal rate from both the anode and the cathode. Separate models for cathode and anode erosions were considered. These models are largely based on the actual experimental observations of several previous researchers on sparking phenomenon in closed chambers. *Expanding circle heat source model (ECHSM) was developed for anode erosion and point heat source model (PHSM) for the cathode erosion.* These two models take into account the fraction of power dis-

tributed between the two electrodes, which in-turn depends upon the electrode materials and dielectric fluid. Therefore *this model takes into consideration the effect of dielectric and the effect of one electrode material over the erosion rate of the other electrode.*

In the present work, the point heat source model (PHSM) is considered as the basis for studying the experimental results for the cathode erosion rates, for few similar materials and dissimilar materials.

1.3 Objective and Scope of the present work

An important consideration in Electric Discharge Machining is to determine the polarity of the electrodes so that the resulting erosion rate of the work is higher than that of the tool. As this may depend upon the pulse on-time, as discussed in Sec1.1 selection of the polarity vis-a-vis the materials of the work and tool electrodes involved needs to be established for each combination. Generally, in die-sinking operation the steel workpiece is connected to the negative polarity. This however, would depend upon the tool electrode material also.

The objective of the present work was therefore chosen to investigate :

1. How the pointed heat source model (PHSM) presented in Sec3.1 can be applied to explain the erosion rate of copper and steel electrodes.

2. How this erosion rate of cathode can be affected by the material of the anode, and

3. whether, for a given tool-work combination the sum-total of the eroded volumes remains invariant with the associated polarities.

The studies were limited to the *mild steel/copper* system.

Chapter 2

EXPERIMENTAL OBSERVATIONS

2.1 Experimental Setup

The EDM machine used was R-35 generator supplied by Electronica, Pune, India. The base unit of the machine supports the discharge cell which contains the dielectric and the fixture to hold the work-piece. A continuous flow of the dielectric was maintained by a pump. The workpiece was mounted in a suitable fixture. The tool electrode was mounted in a collet. Longitudinal feed of the tool electrode was maintained with a servo-motor. The inter-electrode gap was maintained constant with the servo-motor. An electronic weighing machine was used to measure the weight of the tool electrode and the work-piece.

During the trial experiments it was observed that the average current during discharge varies with pulse on-time. The variation is much at low pulse time, however it remains almost constant for higher pulse times. In the present study, average current for each particular pulse time was estimated and has been considered as a dependent parameter.

Nomenclature	Tool(+ve) (anode)	Work-piece(-ve) (cathode)	Figure No.	Remarks
Case A	MS	MS	Fig.2.1,2.2, 2,3,4.2,4.5	Similar electrode materials
Case B	Cu	Cu	Fig.2.4,2.5, 2.6,4.3	
Case C	Cu	MS	Fig.2.7,2.8, 2.9,4.4	Dissimilar electrode materials
Case D	MS	Cu	Fig.2.10,2.11 2.12	

Table 2.1: Electrode pair combinations

2.2 Test and measurement procedure

The tool electrode was connected to the positive terminal and the work-piece to the negative terminal. Side flushing was done to remove the debris from the inter-electrode gap and hence avoid possible short-circuiting. Following were the test conditions used,

Tool size and shape : 5 *mm* diameter cylindrical

Work-piece :

Mild-Steel strip : 25 *mm* $\times$ 25 *mm* $\times$ 8 *mm*(thick)

Copper block: 25 *mm* cube

Dielectric : Kerosene

Discharge voltage : 40 V

Input current : 22 *amp*

Time of machining : 15 - 20 *min* (depending on the test)

Weight loss method was used for estimating the amount of material eroded during a machining operation. The work-piece was mounted on the fixture and tool electrode was held in the collet. Initially the tool was brought down with the help of servo-motor so that it touches the work-piece electrode. To ensure a

constant inter-electrode gap throughout the tool is lifted up to maintain desired inter-electrode gap using a feeler gauge. Dielectric pump was switched on and once the level of dielectric reached above the safe limit indicated by the indicator, supply voltage was impressed across the tool-work gap. The tests were performed for pulse times varying from 2 μsec upto 200 μsec. At each of the pulse times used, the average current was noted down to an accuracy of 1 *amp.* After 15-20 *min* of machining, the weight of both the electrodes was measured with an electronic weighing machine which accurates up-to 0.001 g and hence the amount of material eroded was measured. The erosion rates for an electrode was estimated by dividing the material eroded for that electrode by the duration of machining. *Tests were repeated three times for each* t_{on} *and the average value estimated.*

The above procedure was repeated for four sets of electrode pairs, as shown in Table 2.1. The duty-cycle for all the experiments was kept constant at 10. A calibration chart supplied by the manufacturer (given in appendix A) gives the pulse off-time for different on-times for a particular value of duty cycle. The amounts of material lost are presented in Table 2.2,2.3,2.4 and 2.5 for Case A, Case B, Case C and Case D, respectively.

2.3 Electrode Erosion Rates

2.3.1 Similar Electrode and work Material

Case A (MS/MS system):

Cathode - Mild Steel

Anode - Mild Steel

The experimental observations for the MS/MS system is presented in Table 2.2

Average Current Vs Pulse on-time (MS/MS system)

Fig.2.1 shows the variation of average current with pulse on-time observed in this case when both the electrodes were of mild-steel. In these experimentations,

S.No.	Pulse On-time (μsec)	Pulse Off-time (μsec)	Average Current ($amps$)	Material Removal Rate		Work-tool erosion ratio (WTER)
				MS(-ve) (mm^3/min)	MS(+ve) (mm^3/min)	
1	2	5	3	0.245	0.109	2.24
2	5	7	13	1.129	0.414	2.725
3	10	7	15	1.387	0.518	2.675
4	20	8	15	1.361	0.506	2.687
5	100	22	15	0.779	0.498	1.56
6	200	40	15	0.636	0.445	1.43

Table 2.2: Experimental data for Case A: Cathode - MS; Anode - MS

the current passing through the gap during machining process was found to rise

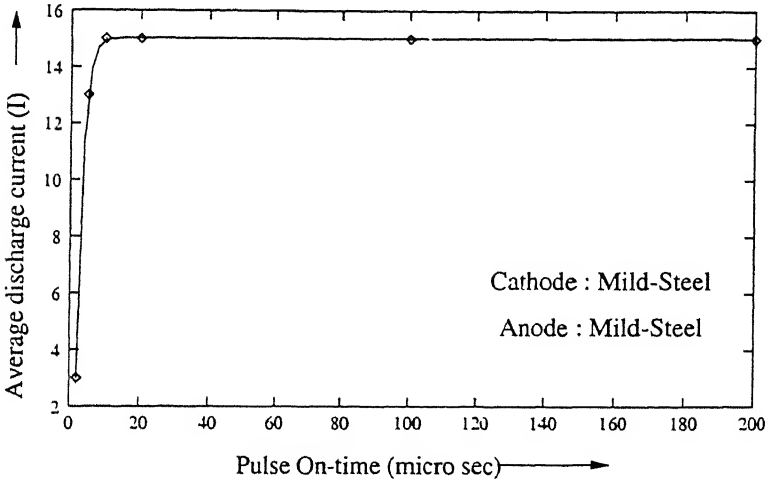

Figure 2.1: Average discharge current for MS(-ve)/MS(+ve)

and stabilizes in accordance with the following ralation of the type $I = a - b\,exp\,(-t_{on}/c)$, value of a, b, c were obtained using the software GNUPLOT (Linux

version 3.5). This is obtained as

$$I = 15.023 - 39.59\ e^{\frac{-t_{on}}{1.678}} \tag{2.1}$$

where t_{on} is measured in μsec and I in amp.

Electrode Erosion rates (MS/MS system)

The variation of the estimated cathode and anode erosion rates against the pulse on-time is shown in the Fig.2.2. A least mean square error fit is obtained using a second order polynomial for the erosion rates of both cathode and anode against log of pulse on-time by using the software GNUPLOT (Linux version 3.5). The

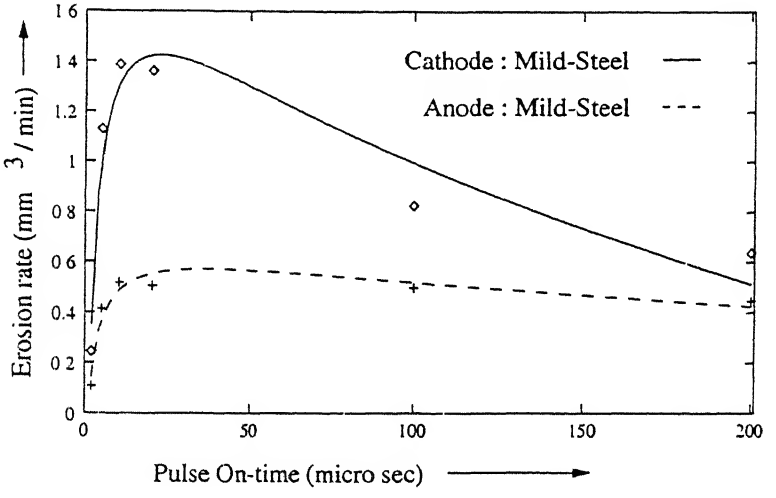

Figure 2.2: Electrode erosion rate for MS(-ve)/MS(+ve) system

erosion rate for the cathode is obtained as

$$\dot{V}_{wc}(Case\ A) = -0.371\ +\ 1.159\ ln(x)\ -\ 0.188\ (ln(x))^2 \tag{2.2}$$

and that for the anode is

$$\dot{V}_{wa}(Case\ A) = -0.09\ +\ 0.368\ ln(x)\ -\ 0.051\ (ln(x))^2 \tag{2.3}$$

This figure depicts the fact that the erosion rate of the cathode (mild-steel) is greater than that of the anode (mild-steel). It appears that the maximum erosion

rate of both the electrodes occurs in the same range of pulse on-time i.e., 20 μsec to 40 μsec. Beyond a certain pulse on-time (typically 40 μsec), the erosion rate of cathode decreases drastically while that of the anode remains more or less constant. It is obvious from these results that *the workpiece (MS) in this case should be connected to the Cathode and the tool (Cu) to the anode.* This indeed is the practice in EDM die-sinking.

Work-Tool Erosion ratio (MS/MS system)

Work-Tool erosion ratio (WTER) i.e., cathode erosion rate / anode erosion rate shown in Fig.2.3 is obtained by fitting a second order polynomial for the experimental data points against log of pulse on-time. This figure shows that WTER remains nearly constant at low pulse times i.e., between 5 μsec and 20 μsec and thereafter it decreases. *In the practical range of operation i.e,, maximum WTER*

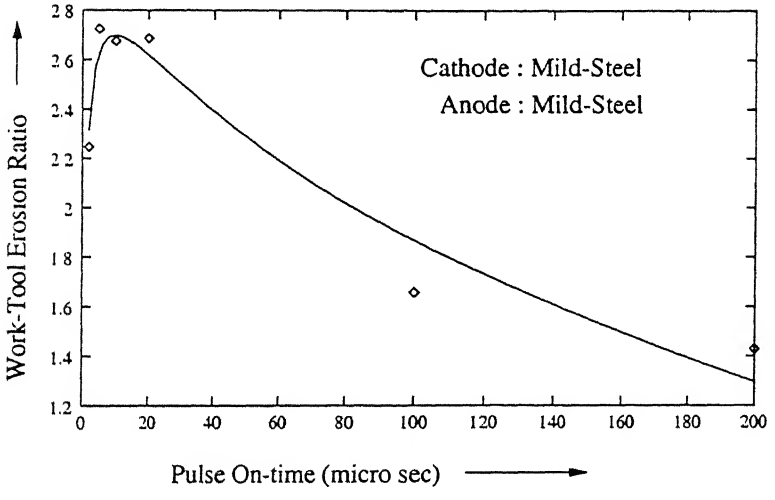

Figure 2.3: Work-Tool erosion ratio for MS(-ve)/MS(+ve)

(between 10 μsec and 30 μsec) which is about 2.6 is quantitatively in agreement with the results of Longfellow et al. [18] (WTER reported by Longfellow is 2.5). For economical use of the process, the WTER should be maximum. Hence, *when both the anode as well as the cathode are of mild-steel, the machining has to be done at lower pulse times.* The inference may be extendable to machining of

S.No.	Pulse On-time (μsec)	Pulse Off-time (μsec)	Average Current ($amps$)	Material Removal Rate		Work-tool erosion ratio (WTER)
				Cu (-ve) (mm^3/min)	Cu (+ve) (mm^3/min)	
1	2	5	3	0.288	0.524	0.533
2	5	7	7	0.661	1.637	0.403
3	10	7	12	1.701	1.823	0.933
4	20	8	14	2.401	1.428	1.681
5	100	22	17	2.557	1.360	1.88
6	200	40	17	1.500	0.914	1.641

Table 2.3: Experimental data for Case B: Cathode - Cu; Anode - Cu

die-steels with softer grades of steel.

Case B (Cu/Cu system)

Cathode - Copper

Anode - Copper

The experimental observations for Cu/Cu system is presented in Table 2.3.

Average Current Vs pulse on-time (Cu/Cu system)

Fig.2.4 shows the variation of average current with pulse on-time when both the electrodes are of copper. As before, the current (I) as a function of pulse on-time (t_{on}) is obtained as

$$I = 16.273 - 16.013\, e^{\frac{-t_{on}}{8.638}} \tag{2.4}$$

where t_{on} is measured in μsec and I in amp.

Electrode Erosion rate (Cu/Cu system)

The variation of the estimated cathode (copper) and anode (copper) erosion rates with pulse on-time is shown in the Fig.2.5. As before, a least mean square error fit is obtained for the erosion rates of both cathode and anode. The erosion rate

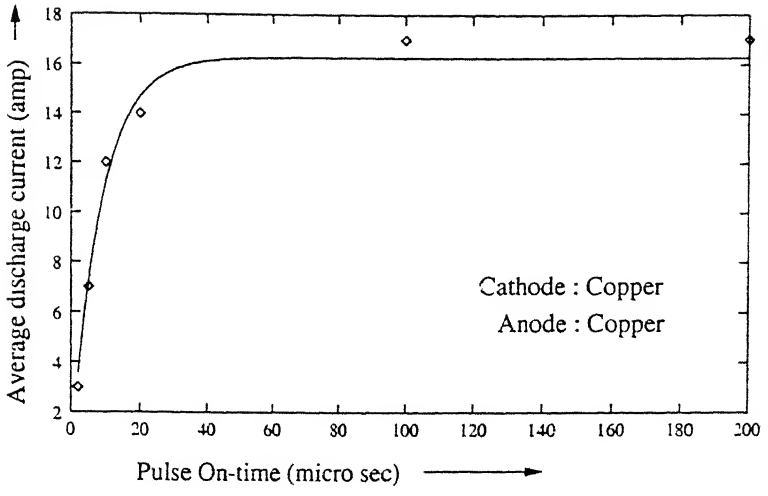

Figure 2.4: Average discharge current Cu(-ve)/Cu(+ve) system

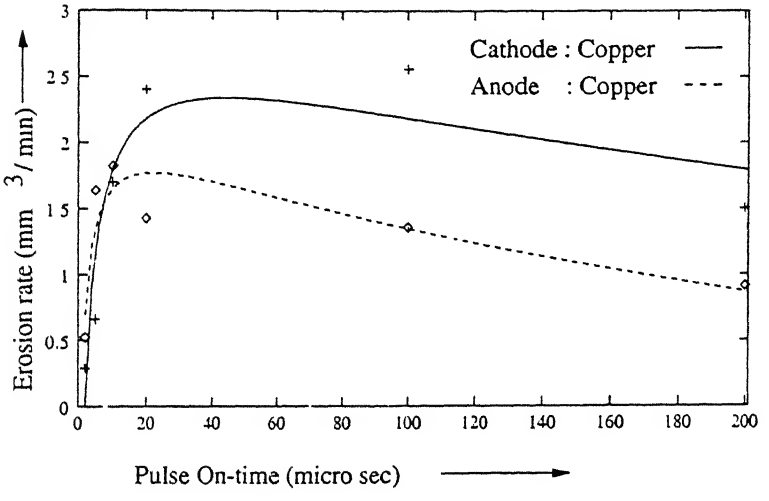

Figure 2.5: Electrode erosion rate for Cu(-ve)/Cu(+ve) system

for the cathode is obtained as

$$\dot{V}_{wc}(Case\ B) = -1.184 + 1.855\ ln(x) - 0.244\ (ln(x))^2 \tag{2.5}$$

and that for the anode is

$$\dot{V}_{wa}(Case\ B) = -0.02 + 1.1548\ ln(x) - 0.186\ (ln(x))^2 \tag{2.6}$$

This clearly shows that at very low pulse on-times (typically less than 5 μsec) only, the erosion rate of anode is more than that of the cathode. This indeed is the

case of wire EDM operation. At all other pulse times the cathode (copper) erodes more than the anode (copper),which is usually the case of die-sinking operation in EDM process. *This trend is in agreement with the results of Heng et al. [20].* The maximum erosion rate of anode occurs at a lower pulse times than that for the cathode. However, beyond about 50 μsec, the erosion rate of both the electrodes(copper) remains almost constant; the erosion rate of cathode being higher than that of anode.

Work-Tool erosion ratio (Cu/Cu system)

The variation of WTER with pulse on-time shown in Fig.2.6 is obtained as in Case A. This clearly shows that the work-tool erosion ratio remains almost constant, (between 80 μsec to 200 μsec) for a wide range of pulse on-time. Therefore

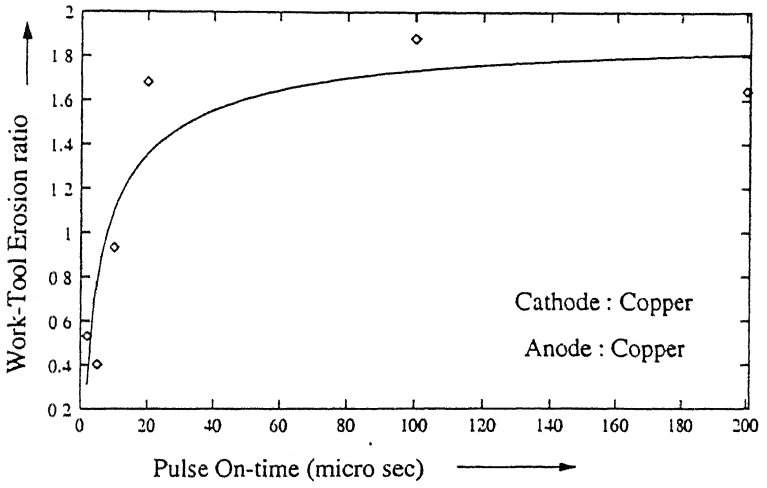

Figure 2.6: Work-Tool erosion ratio Cu(-ve)/Cu(+ve)

for economical use of the process, one will have a wide range of choice of pulse time when both the electrodes are of copper. However the actual set of parameters will depend on other factors. In the practical working range (typically 50 μsec to 100 μsec), *the average value of WTER is about 1.7 which qualitatively agrees with the results of Longfellow et al. [18] (WTER reported by Longfellow is 2.56).* It is to be noted that exact comparison of results should not be expected

S.No.	Pulse On-time (μsec)	Pulse Off-time (μsec)	Average Current ($amps$)	Material Removal Rate		Work-tool erosion ratio (WTER)
				MS (-ve) (mm^3/min)	Cu (+ve) (mm^3/min)	
1	2	5	2	0.9423	0.6902	1.365
2	5	7	6	5.076	2.502	2.028
3	10	7	11	8.328	2.736	3.044
4	20	8	12	11.173	2.702	4.135
5	100	22	13	11.724	1.386	8.459
6	200	40	13	10.312	1.062	9.710

Table 2.4: Experimental data for Cathode - MS; Anode - Cu

because there are number of factors which have an effect on the erosion rate of the electrodes. Some of these are composition and shape of electrodes, duty-cycle, machining area, amount and type of debris, type of generator, composition of dielectric etc [5,7,19,21,24].

2.3.2 Dissimilar electrode materials

Case C ($MS(-ve)/Cu(+ve)$)

Cathode - Mild-Steel

Anode - Copper

The experimental observations for MS/Cu system is presented in Table 2.4.

Average Current Vs **Pulse on-time** (MS/Cu **system)**

The variation of average current (I) as a function of pulse on-time (t_{on}), in this case was observed to vary as shown in Fig.2.7 and is given as

$$I = 12.933 - 15.956\, e^{\frac{-t_{on}}{5.499}} \tag{2.7}$$

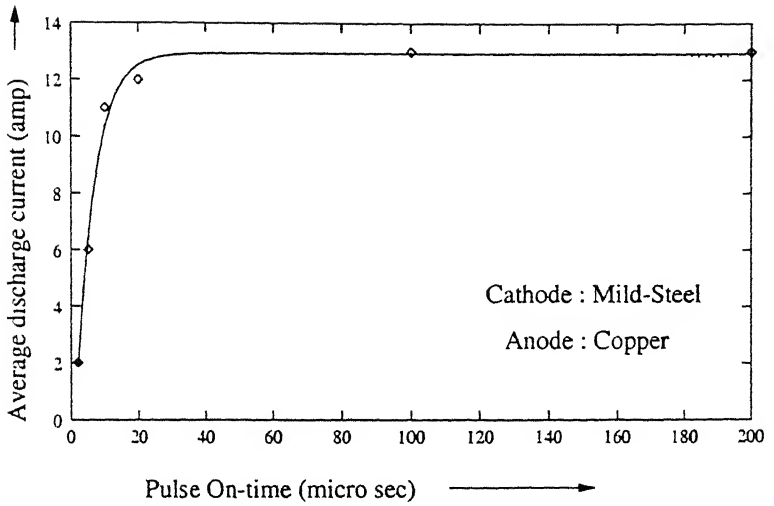

Figure 2.7: Average discharge current MS(-ve)/Cu(+ve) system

where t_{on} is measured in μsec and I in amp.

Electrode Erosion rates (MS/Cu system)

Fig.2.8 depicts the variation of cathode (mild-steel) and anode (copper) erosion rates with pulse on-time. As before a least mean square fit is obtained by considering a second order polynomial for the erosion rates of cathode and anode against log of pulse on-time. The erosion rate of the cathode is obtained as

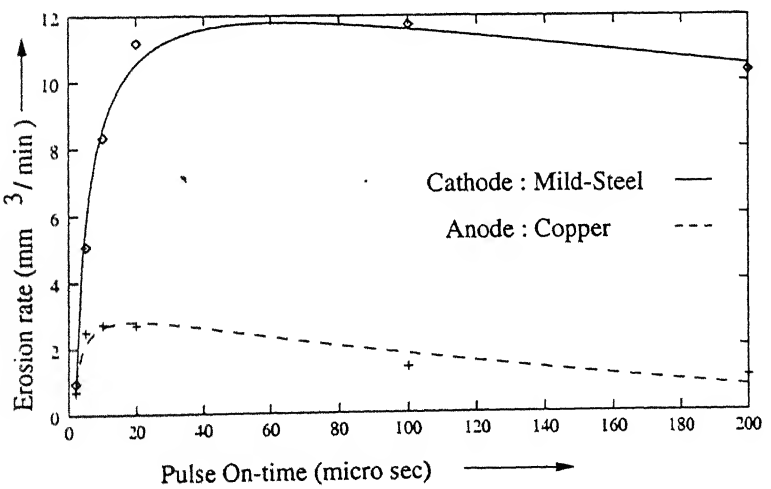

Figure 2.8: Electrode erosion rates for MS(-ve)/Cu(+ve) system

$$\dot{V}_{wc}(Case\ C) = -4.436 + 7.853\ ln(x) - 0.95\ (ln(x))^2 \qquad (2.8)$$

and that for the anode is obtained as

$$\dot{V}_{wa}(Case\ C) = -0.408 + 2.177\ ln(x) - 0.37\ (ln(x))^2 \qquad (2.9)$$

From this figure it is evident that *the erosion rate of the cathode (MS) is always more than that of the anode (Cu).* This is qualitatively in conformity with the results of DiBitonto et al. [14] for iron and Snoeys at al. [17] for die-steel . The erosion rate of anode attains maximum at low pulse times than that of the cathode. Between 5 μsec to 50 μsec the erosion rate of copper (anode) is almost constant while that of mild-steel (cathode) increases. Beyond 50 μsec the erosion rate of both the electrodes decreases.

Work-Tool erosion ratio (MS/Cu system)

The variation of WTER with pulse on-time is obtained as in Case A and is shown in Fig.2.9. From this figure it is clear that the WTER increases with pulse on-time. This qualitatively agrees with the results of George et al. [5] for die-steel. This means that to minimize wear of the tool and at the same time maximize the

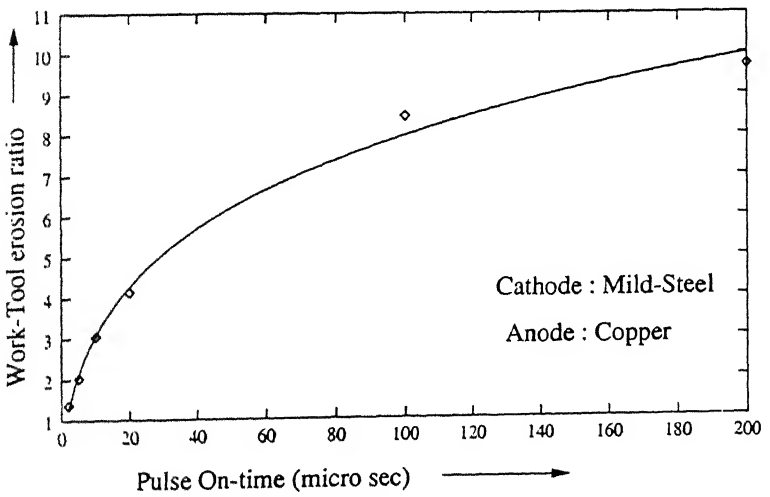

Figure 2.9: Work-Tool erosion ratio for MS(-ve)/Cu(+ve) system

erosion rate of the work-piece, the work-piece (Mild-Steel) should be connected

S.No.	Pulse On-time (μsec)	Pulse Off-time (μsec)	Average Current ($amps$)	Material Removal Rate		Work-tool erosion ratio (WTER)
				Cu (-ve) (mm^3/min)	MS (+ve) (mm^3/min)	
1	2	5	2	0.104	0.23	0.452
2	5	7	9	1.3125	4.632	0.283
3	10	7	13	0.111	0.368	0.302
4	20	8	15	0.058	0.26	0.225

Table 2.5: Experimental data for Cathode - Cu; Anode - MS

to the cathode and tool (Copper) be connected to the anode and machining be done at high pulse time. This indeed is the case with usual die-sinking operation.

Case D (Cu/MS system)

Cathode - Copper

Anode - Mild-Steel

The experimental observations for Cu/MS system is presented in Table 2.5.

Average Current Vs Pulse on-time (Cu/MS system)

Fig.2.10 shows the variation of average current (I) with pulse on-time (t_{on}) obtained as in Sec2.3.1, when the cathode is Copper and anode is Mild-Steel and is given as

$$I = 15.038 - 21.272\, e^{\frac{-t_{on}}{4.056}} \tag{2.10}$$

where t_{on} is measured in μsec and I in amp.

Electrode Erosion rates (Cu/MS system)

The variation of cathode (copper) and anode (mild-steel) erosion rates with pulse on-time is shown in Fig.2.11. The erosion rates of the electrodes were almost negligible beyond 20 μsec pulse time. Hence experiments were not conducted beyond this time. The least mean square error fit in this case could not be

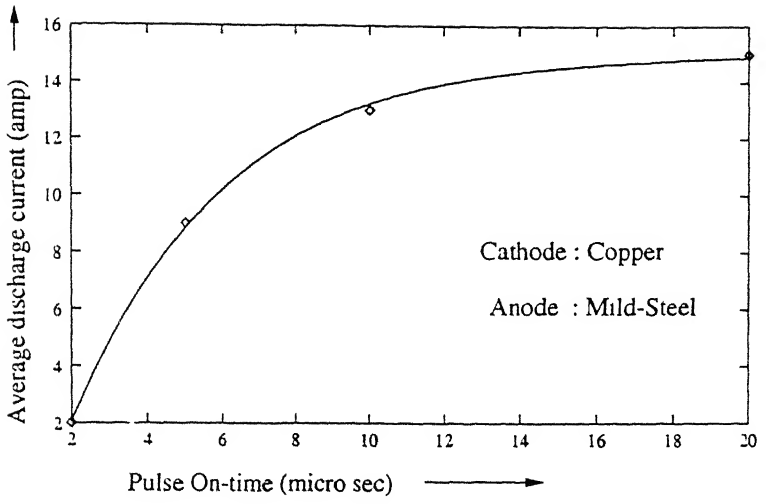

Figure 2.10: Average discharge current for Cu(-ve)/MS(+ve) system

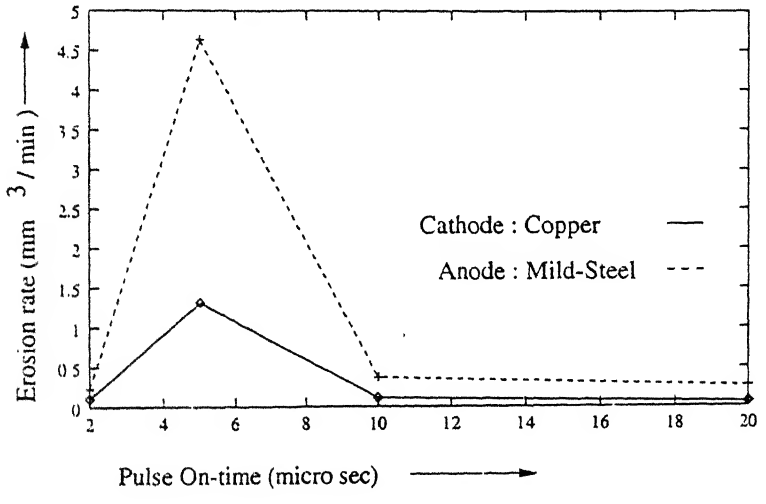

Figure 2.11: Electrode erosion rate for Cu(-ve)/MS(+ve) system

obtained due to lack of enough number of experimental data points. From the Fig.2.11 it is clearly seen that, contradictory to the other cases as shown in Case A, Case B and Case C, *the erosion rate of the anode (Mild-Steel) is more than that of the cathode (Copper).* This trend is in conformity with the results of Albinski [19]. Beyond 10μsec, the erosion rate of the cathode as well as anode is almost negligible. The region 2-10 μsec (see Fig.2.11) provided only 3 machine settings (2 μs,5 μs and 10 μs). Hence the readings corresponding to 5 μsec was

repeated 5 times. By changing the dielectric and other parameters of machining, the scale of erosion rates from the electrodes can be increased. But the general trend is expected to be the same as in Fig.2.11.

Work-Tool erosion ratio (Cu/MS system)

In this case the WTER (cathode erosion rate/anode erosion rate) decreases with increase in pulse on-time as shown in Fig.2.12. However it is very small.

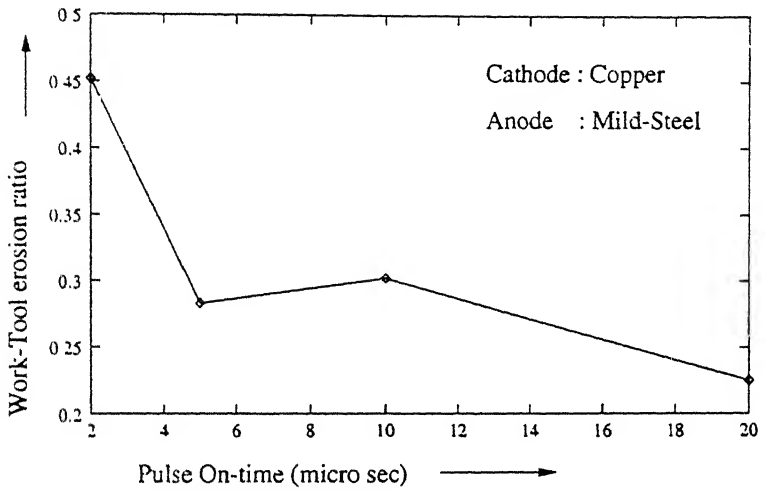

Figure 2.12: Work-Tool erosion ratio for Cu(-ve)/MS(+ve) system

Chapter 3

THEORETICAL ESTIMATES

In the present work an attempt has been made to compare experimentally estimated erosion rates for the cathode with the theoretical estimates obtained using Pointed Heat Source model (PHSM) due to DiBitonto et al. [14].

After carefully studying the features of the EDM process as mentioned in Sec1.1.6, a cathode erosion model, popularly called as pointed heat source model, has been developed by DiBitonto et al. [14] as discussed below.

3.1 Pointed Heat Source Model

Assumptions for the Pointed Heat Source model :

1. There is only one spark per pulse and the plasma radius is very small (< 5 microns).

    - *This is strictly true only for single grain material.*

2. Effective average thermal properties of cathode material apply over the temperature range from solid to liquid melt.

    - *This is obviously to simplify calculations.*

3. A constant fraction (f_c) of the total power (UI) is lost to the cathode, independent of current and pulse time. This fraction may change for different dielectric or electrode materials.

   - *This model does not investigate this aspect at length.*
   - *No proof is available for its validity.*

Fig.3.1 illustrates the spherical symmetry resulting from the above assumptions as well as the melt front radius $R(t)$.

- *This would be true only for a homogeneous single phase material.*

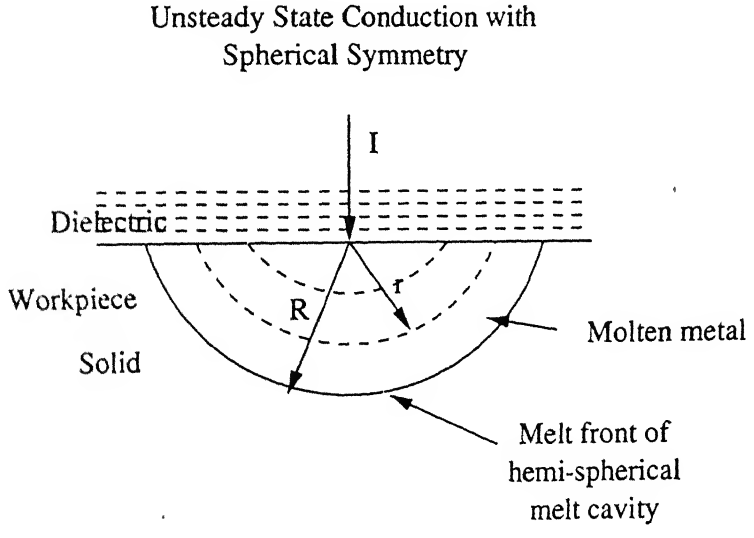

Figure 3.1: Cathode erosion of the pointed heat source model

The governing partial differential equation for this heat conduction problem without heat generation is

$$\frac{1}{\alpha}\frac{\partial T}{\partial t} = \frac{\partial^2 T}{\partial r^2} + \frac{2}{r}\frac{\partial T}{\partial r} \tag{3.1}$$

Here $\alpha \equiv K_T/\rho\, C_p$ is the thermal diffusivity. The associated initial and boundary conditions for the above PDE are

$$IC : t = 0, \forall r, T = T_o, \tag{3.2}$$

$$BC: t > 0, \quad -K_T \frac{\partial T}{\partial r} = q_o, \; for\, r = 0$$
$$-K_T \frac{\partial T}{\partial r} = 0, \; for\, r \neq 0 \tag{3.3}$$

$$BC: t > 0, r = \infty, T = T_o \tag{3.4}$$

where T_o is the ambient temperature of the solid and K_T is the thermal conductivity. The resulting temperature distribution is given by

$$T = T_o + \left(\frac{f_c U I}{2\pi K_T r}\right) erfc\left(\frac{r}{2\sqrt{\alpha t}}\right), \tag{3.5}$$

Equ.3.5 also assumes constant current (I) during the pulse (as EDM machines are usually driven). At the melt radius R,

$$T = T_m = T_o + \left(\frac{f_c U I}{2\pi K_T R}\right) erfc\left(\frac{R}{2\sqrt{\alpha t}}\right), \tag{3.6}$$

which provides $R(t)$.

The melt cavity volume V_c is approximated to be given by

$$V_c = \frac{2}{3}\pi R^3 \tag{3.7}$$

Hence the erosion rate is given by

$$\dot{V}_w = \frac{V_c}{t_{on} + t_{off}} \tag{3.8}$$

3.2 Procedure used to evaluate crater volume of the cathode

The theoretical crater volume can be estimated by simultaneously solving Equ.3.6 and 3.7. Equ.3.6. is used to calculate radius of the crater (R). In this equation it can be seen that all the parameters are either measured or known except f_c i.e., the fraction of power lost to the cathode.

U, I, t_{on} ,T_o are measured parameters during experimentation.

K_T, T_m, C_p and alpha are thermo-physical properties.

The thermo-physical properties of the material [14,15] are given in Table 3.1. Considering the variation of thermo-physical properties over a range of temperature, a set of effective values is used. The ambient temperature (T_o) of the

Material	Density (kg/m^3)	Thermal Conductivity ($W/m\ ^oK$)	Specific heat ($J/kg\ ^oK$)	Thermal diffusivity ($m^2/sec.$)	Melting temperature (^oK)
Mild Steel	7545.0	56.1	575.0	1.293×10^{-5}	1808.0
Copper	8640.0	367.0	438.0	9.698×10^{-5}	1356.0

Table 3.1: Material Properties

material is taken as 298^oK. Average discharge current (I) is taken as a function of pulse on-time as obtained in Equ.2.1, 2.4, 2.7 and 2.10.

DiBitonto et al. [14] have assumed that the factor f_c is constant for a particular electrode pair and dielectric. They have estimated f_c on the basis of optimum pulse time by tuning the theoretical optimum pulse time with the measured values by AGIE corporation corresponding to 42 μsec pulse time and hence calculated the theoretical optimum pulse times and corresponding erosion rates. Their results have shown a good agreement between the theoretical and optimum pulse time. But the flushing efficiency, i.e., ratio of experimental estimates to the theoretical estimates, have been found to decrease with decrease in pulse times. Their results have shown decrease in flushing efficiency, i.e., ratio of difference of theoretical and experimental estimates with the experimental estimates, with decrease in optimum pulse times.

In the present work, it is assumed that f_c is a function of energy input, the reason for which is justified in Sec3.4. Therefore as a first degree of approximation,

a linear variation of f_c with energy input into the system, is considered to be applicable.

3.3 Calculation of theoretical crater volume

Theoretical crater volume is calculated as follows. Initially f_c as a linear function of energy input is obtained by obtaining f_c corresponding to the pulse times 5 μsec and 200 μsec (points P_i and P_f in Fig. 4.2, 4.3 and 4.4) as explained below.

In the actual machining process, multiple discharges per spark occur which result in multiple craters. Therefore for the theoretical calculations, which assume single discharge per spark (assumption no. 1) and hence single crater, the *equivalent crater* corresponding to the sum of all multiple craters in the actual process is taken. The radius corresponding to this crater is called as the equivalent crater radius and the crater volume as equivalent crater volume.

Equivalent crater radius (R) for the pulse on-times 5 μsec and 200 μsec is obtained by substituting equivalent crater volume, i.e., experimental, corresponding to these two pulse on-time in Equ.3.7. These two pulse on-times are chosen because the theoretical crater volume is calculated between these two limits and compared with the experimental results. Hence f_c is obtained by substituting the obtained equivalent crater radius in Equ.3.6. Since U, I and t_{on} are known at these two points, a linear function of f_c with energy input (UIt_{on}) into the system is obtained. This is done for Case A, Case B and Case C and is given in Equ.3.9, 3.10 and 3.11, respectively.

$$f_c \text{ (CaseA)} = 0.0068 + 0.025(UIt_{on}) \tag{3.9}$$

$$f_c \text{ (CaseB)} = 0.0464 + 0.111(UIt_{on}) \tag{3.10}$$

$$f_c \text{ (CaseC)} = 0.0329 + 0.065(UIt_{on}) \tag{3.11}$$

The crater radius in Case D is so low that the convergence of Equ.3.6 could not

be obtained and hence f_c in this case is not calculated. The results of the present work show that f_c in Case A i.e., MS(-ve)/MS(+ve) system varies from 0.0068 to 0.0098 (see Equ.3.9). This qualitatively agrees with the results reported elsewhere [2] which shows the fraction of energy going to MS as cathode varies from 0.006 to 0.002 when the current is varied from 10 to 40 amp at 20 V discharge voltage.

Now the theoretical crater radius is obtained to an accuracy of 0.1 μm by substituting the obtained f_c as a function of energy in Equ.3.6 and obtaining the convergence for different pulse times. Hence the theoretical crater volume is obtained by substituting the crater radius (R) in Equ.3.7. This is done for all the three cases i.e., Case A, Case B and Case C.

The experimental equivalent crater volume is given by the product of erosion rate and pulse time (pulse on-time + pulse off-time).

3.4 Justification for variable f_c as function of energy input

The distribution of energy into the system elements i.e., cathode, anode and the dielectric in EDM process is very complex [2,6,7,14,15]. However a simplified analysis of the process reveals that, for a given energy input per pulse at the inter-electrode gap, the fraction of energy lost to the electrodes depends upon the quantity of energy supplied per pulse at the inter-electrode gap. This is explained as below.

The nature of variation of distribution of energy to the electrodes with the energy supplied per pulse appear to occur in three stages as discussed below.

Stage 1: At lower energies, most of the energy will be lost in ionisation, excitation and formation of plasma channel. Therefore the fraction of energy lost to the electrodes will be less.

Stage 2: With further increase in energy at the inter-electrode gap, obviously the

energy component conducted into the electrodes will increase.

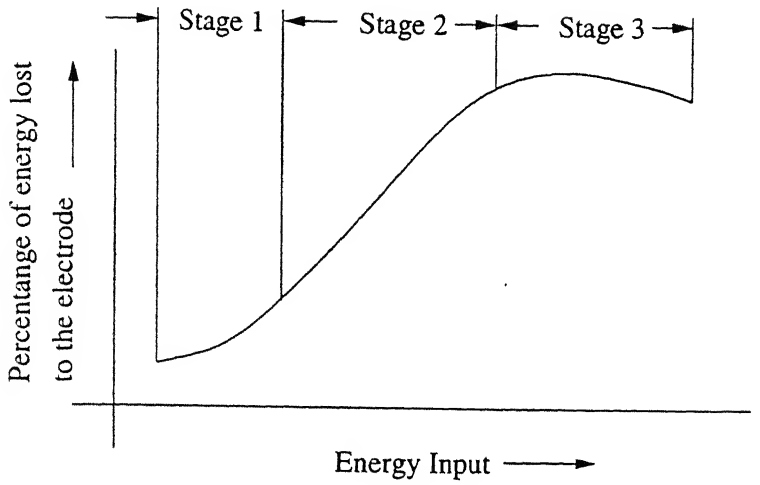

Figure 3.2: Component of energy lost to the electrodes

Stage 3: However a further increase in energy does-not give a significant increase in the fraction of energy conducted to the electrodes because the additional energy supplied will be lost in maintaining the plasma channel, further melting of the molten material, and evaporation of the dielectric fluid [6]. Obviously with further increase in energy, the fraction of energy lost to the electrodes will decrease.

The above discussion can be summarized as shown in Fig.3.2. The fraction of power lost to the cathode (f_c) in Equ.3.6 is identical to the fraction of energy lost to the electrodes. Hence, from the above discussion it is justified that the *fraction of power lost to the cathode is a function of energy supplied at the inter-electrode gap.*

Chapter 4

RESULTS AND DISCUSSION

4.1 Average Discharge Current

Fig.4.1 shows the variation of average current with pulse on-time during a discharge observed in all the four cases (see Table 2.1). In all the four cases, the nature of variation of average current with pulse on-time is similar i.e., it first increases rapidly and after about 20 μsec remains nearly constant. On changing the electrode material and polarity of the electrodes, the average current changes, when all the other machining condition are kept the same. Since the average current results due the flow of electrons at the inter-electrode gap, it can be said that *the resistance to the flow of electrons changes with change in electrode material and polarity.* Upto 20 μsec, the resistance to the flow of electrons appears to follow the order as shown below.

Case C > Case B > Case D > Case A

However, beyond about 20 μsec, the order of resistance to the flow of electrons is

Case C > Case A > Case B

(the current in Case D beyond 20 μsec is not measured because the erosion rates were very low beyond this pulse time).

This means that the *energy impressed* (UIt_{on}) *at the inter-electrode gap depends on the electrode material and polarity of the electrodes.*

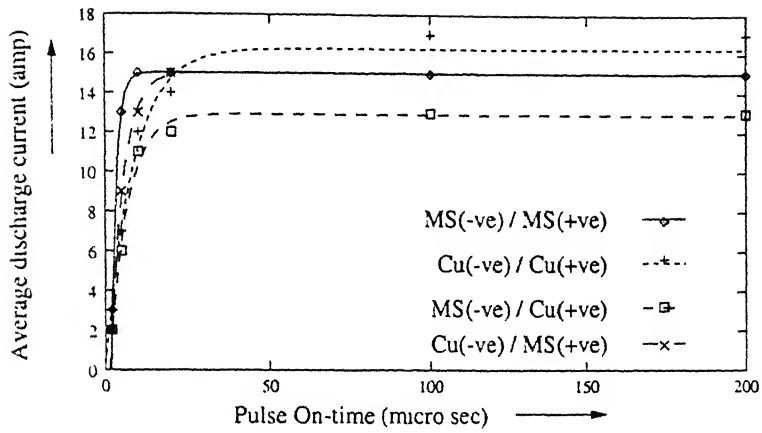

Figure 4.1: Average discharge current

4.2 Comparison of theoretical and experimental results for cathode erosion

The theoretical crater volume obtained in Sec3.3 together with the experimental crater volume are shown for Case A, Case B and Case C in Fig.4.2, Fig.4.3 and Fig.4.4, respectively. It is clearly seen from these figures that the theoretical crater volumes are closer to the experimental crater volumes except for Case A (Fig.4.2). Hence for Case A, f_c as a function of second order polynomial of energy input is obtained by obtaining f_c corresponding to 100 μsec pulse on-time. This is given as

$$f_c = 0.0067 + 0.099(UIt_{on}) - 0.6096(UIt_{on})^2 \tag{4.1}$$

Now the crater volume is calculated as before and plotted along with experimental crater volume as shown in Fig.4.5. This figure shows that the theoretical crater volume is very close to the experimental crater volume. This is explained as follows.

For a given energy input at the inter-electrode gap, it is logical to assume that the volume of the equivalent crater formed at the cathode will be proportional to the energy impressed at the cathode. The fraction of total energy at inter-

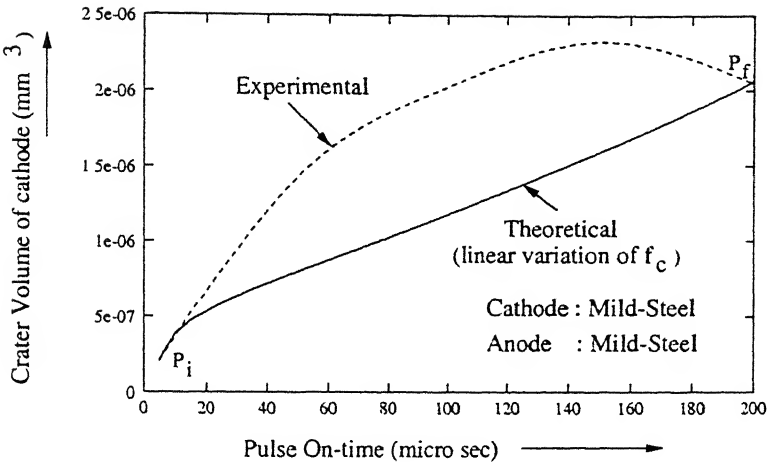

Figure 4.2: Crater volume for MS(-ve)/MS(+ve) system (first order variation of fc)

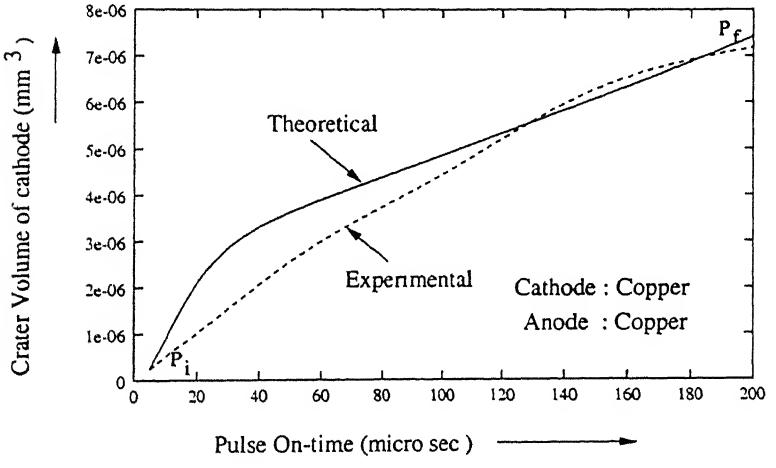

Figure 4.3: Crater volume for Cu(-ve)/Cu(+ve) system

electrode gap lost to the cathode, i.e., energy impressed at the cathode, is identical to the fraction of power lost to the cathode. This means that the trend of variation of the crater volume will be similar to that of the variation of f_c with energy input into the system. The experimental crater volume in Case B and Case C (see Fig.4.2 and Fig.4.3) almost varies linearly within the given range of pulse time. This means that the *stage 3* (see Fig.3.2) is not reached for the given range

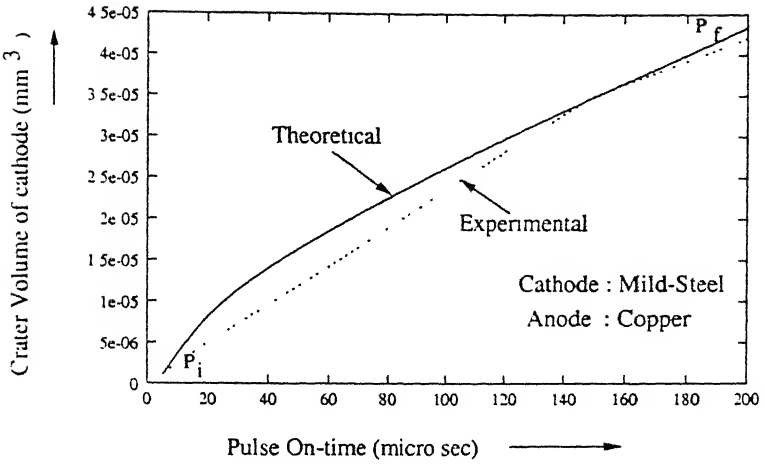

Figure 4.4: Crater volume for MS(-ve)/Cu(+ve) system

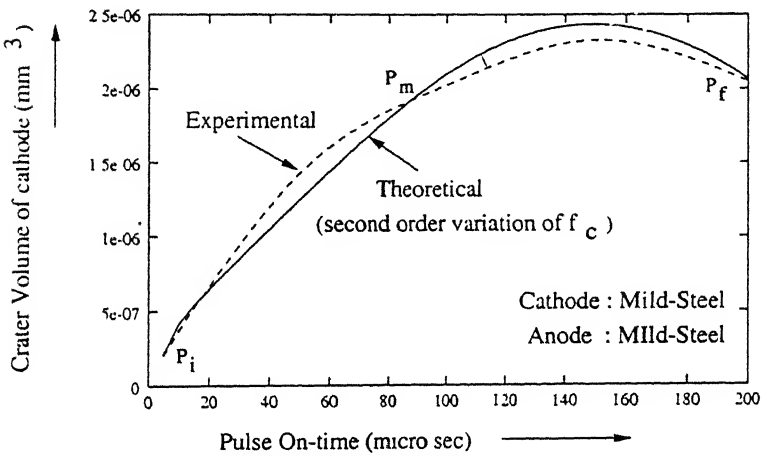

Figure 4.5: Crater volume for MS(-ve)/MS(+ve) system (second order polynomial of fc)

of energy input into the system. Therefore variation of f_c with energy input into the system upto the *stage 2* (see Fig.3.2) can be considered as a first degree of approximation, to be a linear variation. Hence the theoretical crater volume calculated by assuming a linear variation of f_c with energy input into the system resulted in very close agreement to the experimental crater volume. However, in Case A, the experimental crater volume increases up-to 150 μsec and there

after it decreases. This means that the *stage 3* (see Fig.3.2) has been reached for the given range of energy input in this case i.e., when the cathode as well as the anode material is of Mild-Steel. Therefore it is appropriate to approximate f_c as a second order polynomial of energy input. Hence the theoretical crater volume calculated by assuming a second order variation of f_c with energy input into the system resulted in very close agreement to the experimental values(see Fig.4.5).

The above results show that the PHSM developed by DiBitonto et al. [14] can be used to estimate the erosion rate of cathode with a fair degree of accuracy, provided we obtain f_c *as a function of energy input into the system for a particular cathode and anode pair.* However, a logical and fundamental basis is required for estimation of f_c for a given set of experimental parameters. f_c should actually be determinable from the physics of the problem, but that is obviously not very straight forward.

4.3 Sum of cathode and anode erosion rates

4.3.1 Similar electrode materials (Case A and Case B)

The sum of erosion rates of the electrodes (cathode + anode) for the two cases, Case A (MS/MS system) and Case B (Cu/Cu system) is shown in Fig.4.6. The sum of erosion rates of the electrodes in both the cases i.e., MS/MS and Cu/Cu system increases upto certain pulse energy (typically $12mJ$) and there after it decreases. However, it can be seen that the sum of erosion rates in Cu/Cu system is greater than that in MS/MS system. If the PHSM due to DiBitonto et al. [14] is accepted to be applicable as stated in Sec4.2, then the only possible explanation is that for a given energy input, *the fraction of energy lost to the two electrodes is more for Cu/Cu system than MS/MS system.* This can be seen from Equ.3.9 and Equ.3.10. The difference in the erosion rates will also be due to change in the thermal properties of the electrode material. The crater volume for Mild-Steel

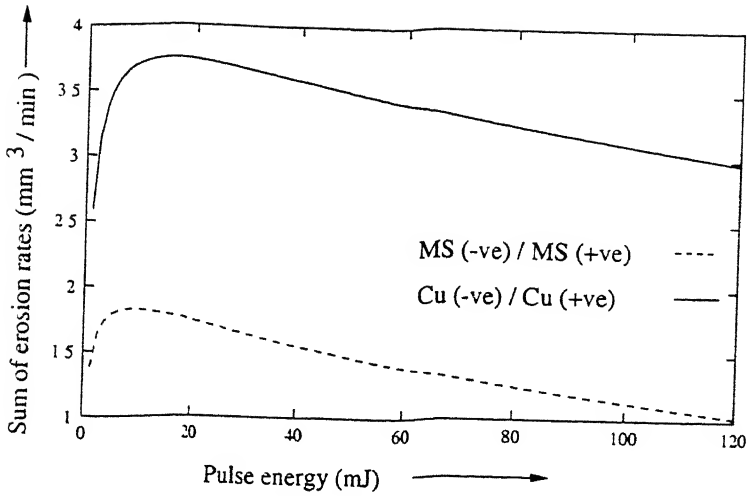

Figure 4.6: Sum of erosion rates of MS/MS and Cu/Cu system

as well as Copper calculated by Equ.3.6 and Equ.3.7 for a constant value of f_c (0.02) and plotted in Fig.4.7. This figure shows that the erosion rate of *Mild-Steel is greater than that of Copper.* This difference in erosion rates is due to the

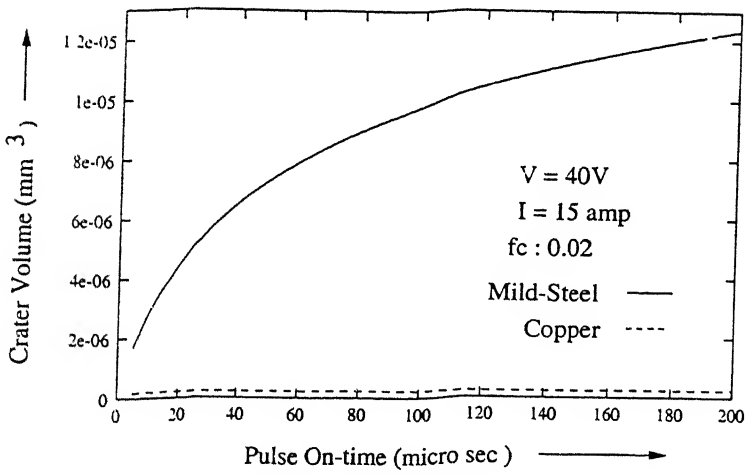

Figure 4.7: Crater volume of MS and Cu for fc : 0.02

thermal properties of the electrode material. But in the actual case (see Fig.4.6) *the erosion rate of Copper is greater than that of Mild-Steel* for a given energy input. This clearly shows that the factor f_c which is much greater in Cu/Cu

system than MS/MS system has a dominant effect in increasing the erosion rate of the electrodes in Cu/Cu system.

4.3.2 Dissimilar electrode materials (Case C and Case D)

The sum of erosion rates of the electrodes in Case C ($MS(-ve)/Cu(+ve)$ system) and Case D ($Cu(-ve)/MS(+ve)$ system) is shown in Fig.4.8. As in the earlier

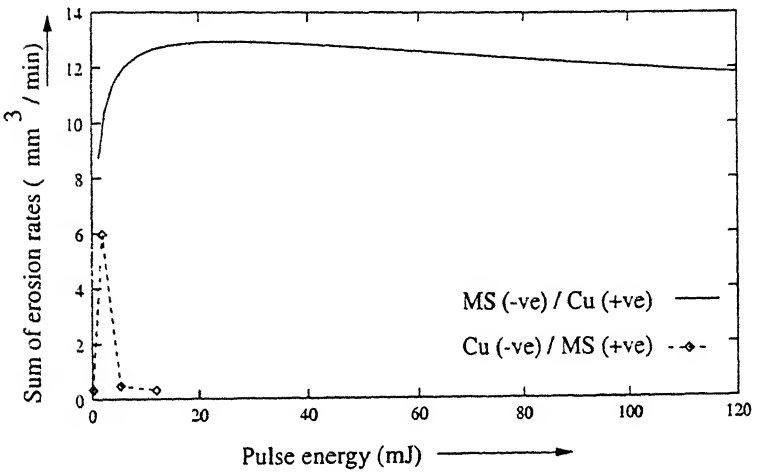

Figure 4.8: Sum of erosion rates of MS(-ve)/Cu(+ve) and MS(+ve)/Cu(-ve) system

case, the sum of erosion rates of both the electrodes increases upto certain pulse energy and there after it decreases. The decrease in sum of erosion rates in Case D i.e., when the cathode is Copper and anode is of Mild-Steel is very steep after 1.8 mJ of energy. But beyond 12 mJ the sum of erosion rates is negligible. However in Case C i.e., when the cathode is Mild-Steel and anode is Copper, the rate of decrease of sum of erosion rates beyond 10 mJ is very low. It may be noted that the erosion rates beyond 20 μsec (see Fig.2.11) in Case D could not be calculated due to extremely low erosion rates of the cathode. This means the component of energy lost to the cathode is very low. The low erosion rates of the anode signifies that the fraction of energy lost to the anode is also very low.

Therefore, in Case D the component of energy distributed at the electrodes is very low and hence low sum of erosion rates. But in Case C, the sum of erosion rates is much greater than in Case D. This is because *the component of energy lost to the electrodes in Case C is much greater than in case D.*

In both the above cases (Sec4.3.1 and Sec4.3.2), the sum of erosion rates decreases beyond certain pulse energy. This may be due to the following reason.

At high pulse energies, in-order to keep the breakdown field constant, the electrode gap spacing increases. This results in higher amount of heat loss, radial diffusion of ions and redeposition between cathode and the anode. Therefore the component of energy distributed at the electrodes decreases. Hence the amount of material eroded from both the electrode decreases which results in the decrease in the sum of erosion rates of the electrodes at high pulse energies.

4.4 Polarity effect

The only difference in Case C and Case D is the polarity of the electrodes. This change in polarity has resulted in a huge difference in the erosion rates of the electrodes (see Fig.2.8 and Fig.2.11). The sum of erosion rates of the electrodes in Case C is also much greater than in Case D as discussed in Sec4.3.2 (see Fig.4.8).

The energy supplied at the inter-electrode gap is lost into the system elements (i.e., cathode, anode, and dielectric), radiation and some other forms of energy. This can be written as

$$\begin{aligned} \text{Total energy input}(E) &= E_e + E_w + E_d + E_r \\ \Rightarrow 1 &= \frac{E_e}{E} + \frac{E_w}{E} + \frac{E_d}{E} + \frac{E_r}{E} \\ \Rightarrow \quad 1 &= f_c + f_a + f_d + f_r \end{aligned} \tag{4.2}$$

If material removal from an electrode pair in a given dielectric is independent

of the polarity of the electrodes then changing the polarity should not alter the sum of erosion rates. But Fig.4.8 shows clearly that when the polarity of Cu is changed, the total erosion volume changes drastically. This is more for MS(-ve)/Cu(+ve) system than Cu(-ve)/MS(+ve) system. Therefore from Equ.4.2, we have

$$\text{for Case C,} \quad 1 = (f'_c + f'_a) + f'_d + f'_r$$
$$\text{and for Case D,} \quad 1 = (f''_c + f''_a) + f''_d + f''_r$$

Concluding from Fig.4.8, therefore

$$(f''_c + f''_a) < (f'_c + f'_a) \tag{4.3}$$

Now, if radiation and other forms of losses which are not accounted for are same in both the cases i.e., $f'_r = f''_r$, then obviously $f''_d > f'_d$. This implies that more energy is available in the dielectric media. This should result in higher temperature rise of the dielectric in Case D. This investigation was not taken up in the course of present work and is suggested as a future task.

On the other-hand if the energy lost to the dielectric is same in both the cases i.e., $f'_d = f''_d$, then $f''_r > f'_r$ i.e., radiation losses and other losses which are not accounted for has to be higher in Case D (when the cathode is Cu) than in Case C. This aspect can be investigated by resorting to measurement of energy due to ultra-violet, infra-red and visible light in the discharge and is proposed as a future task.

4.5 Influence of Anode material on the erosion rates of the cathode material

The variation of the erosion rates of the cathode material with different anode material has been studied in two cases as discussed below.

4.5.1 Erosion rate of Mild-Steel as cathode material with different anode material

Comparison of Case A and Case C

Cathode : Mild-Steel

Anode : Mild-Steel, Copper

From Table 2.1 it can be seen that the cathode material in both Case A and Case C is Mild-Steel while the anode is Mild-Steel and Copper, respectively. In both the cases, the erosion rate of the cathode is more than the erosion rate of the anode (see Fig.2.2 and Fig.2.8). The erosion rates of the cathode in these two combinations of electrode pair is shown in Fig.4.9. It can be seen from

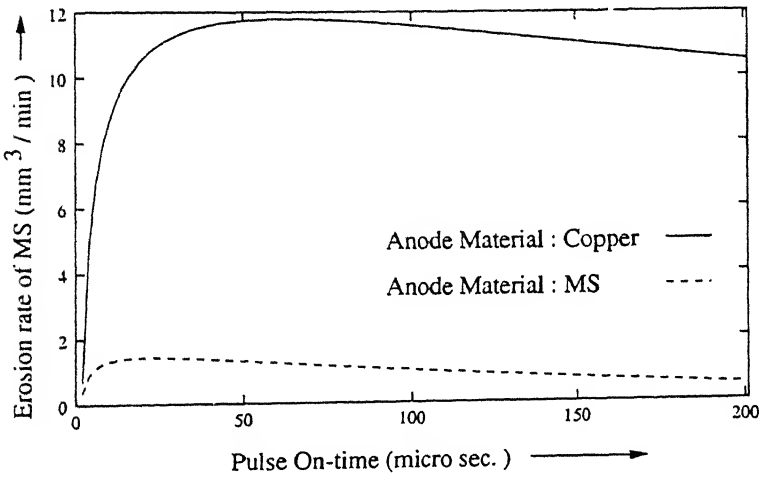

Figure 4.9: Erosion rate of MS (Cathode) when the Anode material is MS and Cu

Fig.4.9 that the erosion rate of Mild-Steel increases by about 10 times when the anode material is changed from Mild-Steel to Copper. *This shows that when the anode material is Copper, greater fraction of power is lost to the cathode (Mild-Steel) than when the anode material is Mild-Steel.* The mechanism of erosion, energy distribution and dynamics of plasma may not be exactly identical. The erosion rate of the cathode (Mild-Steel) becomes maximum at higher pulse times

when the anode is of Copper than when it is Mild-Steel. The decrease in the erosion rate after the optimum pulse time is low in Case C, whereas the erosion rate decreases drastically in Case A after optimum pulse time. In practice, in addition to maximum material removal rate, the selection of tool depends upon many other factors, the most important of which is work-tool erosion ratio. This factor becomes more important when the manufacturing of the tool is very costly or high accuracy of machining i.e., minimum erosion of tool, has to be maintained. This means that the work-tool erosion ratio should be maximum. The work-tool erosion ratio decreases after a certain pulse time, typically 10 μsec, when the anode is Mild-Steel (see Fig.2.3) whereas it increases when the anode is of Copper (see Fig.2.9). However, the WTER in Case C i.e., when anode is Copper, is much greater than that in Case A i.e., when anode is Mild-Steel. Therefore when the interest is of high erosion rate of Mild-Steel and at the same time maintain high accuracy of machining, Copper should be prefered to Mild-Steel as anode (tool) and the machining be done at high pulse times. This inference may be extended to machining of die-steels.

However for high surface finish of the work-piece (Mild-Steel), the combination which gives lower erosion rates should be prefered i.e., the Mild-Steel may be prefered to Copper for the tool (anode). Further work on this aspect is suggested.

4.5.2 Erosion rate of Copper as cathode material with different anode material

Comparison of Case B and Case D

Cathode : Copper

Anode : Copper, Mild-Steel

From Table 2.1 it can be seen that the cathode in both the Case B and Case D is Copper while anode is of Copper and Mild-Steel respectively. In Case B, upto about 5 μsec (see Fig.2.5), the erosion rate of cathode(Copper) is very close to

that of the anode (Copper); the difference in the erosion rates being negligible. But after about 5 μsec, the erosion rate of the cathode is much more that of the anode. In Case D (see Fig.2.11), the erosion rate of anode (Mild-Steel) is more than that of the cathode (Copper) for the whole range of pulse times. The erosion rate of cathode (copper) in these two combinations of electrode pair i.e., Case B and Case D is shown in Fig.4.10.

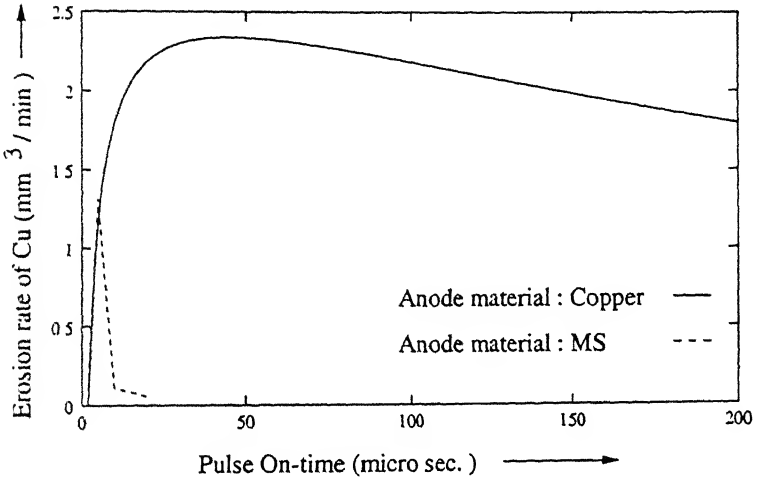

Figure 4.10: Erosion rate of Cu(Cathode) when the Anode material is MS and Cu

It can be seen from Fig.4.10 that the erosion rate of Copper is negligible after 10 μsec when the anode is of Mild-Steel. The erosion rate of cathode (Copper) almost follows the similar curve up-to 5 μsec in both the cases. However, beyond that the erosion rate of the cathode (Copper) is significantly more when the anode is of Copper than Mild-Steel. This clearly shows that *the fraction of power lost to the cathode (Copper) is much more when the anode is also of Copper than Mild-Steel.* The erosion rate of cathode (copper) attains maximum at higher pulse times when the anode is of Copper rather than Mild-Steel. The erosion rate decreases drastically between 5 μsec to 20 μsec and thereafter remains almost negligible when the anode is of Mild-Steel. However, the rate of decrease of erosion rate

of the cathode (Copper) when the anode is of Copper is relatively lower. The work-tool erosion ratio decreases when the anode is of Mild-Steel (see Fig.2.12) whereas it increases when the anode is of Copper (see Fig.2.6) with pulse on-time. However the WTER in Case B increases rapidly only upto certain pulse on-time and beyond that the rate of increase is less. Therefore, for high erosion rate and at the same time maintain high accuracy of the machining of Copper, Copper should be preferred to Mild-Steel as anode and machining can be done for a wide range of pulse on-time (typically 80 μsec to 200 μsec).

From the discussion in Sec4.5.1 and Sec4.5.2 it can be said that by changing the anode material, the erosion rates of the cathode can be changed drastically. *Copper as anode results in greater fraction of power lost to the cathode (Cu or MS) when compared to Mild-Steel as anode.* This brings out a significant role of Cu as an electrode. Besides the usual thermal properties of Cu, its fundamental electronic properties like work function, fermi energy, emissivity etc may be of significance. This could influence the erosion mechanism. Therefore for the economical machining (high material removal rate) of Mild-Steel or Copper, the work-piece should be connected to the cathode and Copper be preferred to Mild-Steel for tool (anode).

4.6 Influence of Cathode material on the erosion rates of the Anode material

The variation of the erosion rates of the anode material with different cathode material has been studied in two cases as discussed below.

4.6.1 Erosion rate of Mild-Steel as anode material with different cathode material

Comparison of Case A and Case D

Anode : Mild-Steel

Cathode : Mild-Steel, Copper

From Table 2.1 it can be seen that the anode material in Case A and Case D is Mild-Steel while the cathode is Mild-Steel and Copper, respectively. In Case A i.e., when the cathode is Mild-Steel, the erosion rate of anode (Mild-Steel) is less than that of the cathode (see Fig.2.2). But when the cathode material is changed from Mild-Steel to Copper, the erosion rate of the anode is more than that of the cathode (see Fig.2.11). The erosion rates of anode (Mild-Steel) in these two pair of electrode material combination is shown in Fig.4.11.

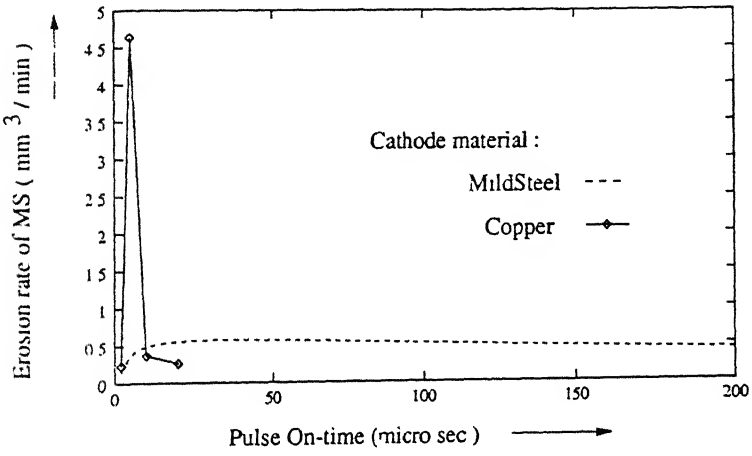

Figure 4.11: Erosion rate of MS(Anode) when the Cathode material is MS and Cu

Upto 10 μsec the erosion rate of the anode (Mild-Steel) is more when the cathode is Copper. But beyond 10 μsec, Mild-Steel as Cathode erodes more material from anode (Mild-Steel) than Copper as cathode. The erosion rates of the anode becomes almost negligible beyond 20 μsec when the cathode is Copper. However the rate of decrease of erosion rates of the anode (Mild-Steel) is very low beyond optimum pulse time (typically 20 μsec) when the cathode material is Mild-Steel.

4.6.2 Erosion rate of Copper as anode material with different cathode material

Comparison of Case B and Case C

Anode : Copper

Cathode : Mild-Steel, Copper

From Table 2.1 it can be seen that the anode material in both Case B and Case C is Copper while cathode is of Mild-Steel and Copper respectively. The erosion rate of anode (Copper) is less than that of the cathode when the cathode is either Mild-Steel or Copper (see Fig.2.5 and Fig.2.8). However Fig.4.12 clearly shows that the magnitude of the erosion rates of the anode (Copper) varies considerably when the cathode is changed from Mild-Steel to Copper.

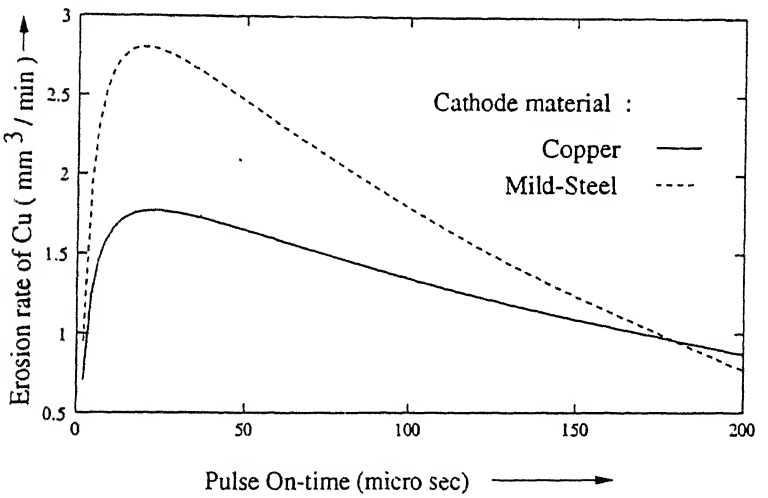

Figure 4.12: Erosion rate of Cu(Anode) when the Cathode material is MS and Cu

Mild-Steel as cathode material results in greater erosion from the anode (Copper) for a wide range of pulse on-time when compared to Copper as cathode material. However beyond 180 μsec, copper as cathode results in more material removal from the anode (Copper) than Mild-Steel as cathode. Material removal rate of Copper (anode) attains maximum at low pulse times when the cathode

is either Copper or Mild-Steel. However the decrease in material removal rate of the anode(Copper) is more steep when the cathode material is Mild-Steel when compared to that when the cathode material is Copper.

From the results discussed in Sec4.6 and Sec4.7 it can be said that for a given energy input into the system, *the fraction of power lost to one electrode depends strongly on the other electrode material.* This factor is responsible for the change in erosion rate of one electrode (cathode or anode) when the other electrode material (anode or cathode) is changed.

Chapter 5

CONCLUSIONS

5.1 Conclusions

In the present work, electric discharge machining on four sets of electrode pair i.e., MS(-ve)/MS(+ve), Cu(-ve)/Cu(+ve), MS(-ve)/Cu(+ve) and Cu(-ve)/MS(+ve), has been carried out and the following conclusions have been derived.

1. In MS(-ve)/MS(+ve), Cu(-ve)/Cu(+ve) and MS(-ve)/Cu(+ve) system, the erosion rate of the cathode is more than that of anode. But in Cu(-ve) / MS(+ve) system, the erosion rate of anode is greater than the cathode. This may be due to the difference in distribution of energy at the cathode and anode, for a given set of parameters, which depends upon the electrode material and polarity of the electrodes.

2. The PHSM due to DiBitonto et al.[14] has been studied with the experimental results for four sets of electrode pair. The experimental results have been compared with the results of other researchers whereever possible. It has been concluded that the PHSM can be used to predict the erosion rate of the cathode, for a given electrode pair, with a fair degree of accuracy provided we obtain the factor f_c as a function of energy input into the system.

3. Greater component of pulse energy is transmitted to the electrodes in the Cu(-ve)/Cu(+ve) system than in MS(-ve)/MS(+ve) system. This means that the loss of energy into the dielectric and other forms of radiation energy such as ultra-violet, infra-red, visible light etc is more in MS(-ve)/MS(+ve) system than in Cu(-ve)/Cu(+ve) system.

4. The study has shown that an electrode (anode or cathode) has a significant effect on the distribution of energy at the other electrode (cathode or anode). Copper as anode results in greater fraction of energy distributed at the cathode (MS or Cu) when compared to MS.

5. Polarity of the electrodes has a significant effect on the distribution of energy into the system elements. The energy transmitted to the electrodes in MS(-ve)/Cu system is *significantly greater* than that in the Cu(-ve)/MS system. Hence it has been postulated that the energy lost into the dielectric will be more in Cu(-ve)/MS system than in MS(-ve)/Cu system. This may result in much increase in temperature of the dielectric in Cu(-ve)/MS system than in MS(-ve)/Cu system.

5.2 Scope for future work

1. The electrode material properties which influence the distribution of energy into the electrodes with change in polarity has to be studied. Then a theoretical model can be developed to obtain the fraction of power distributed at the electrodes as a function of energy input into the system, polarity of the electrodes and electrode material properties.

2. The temperature of the dielectric can be investigated for different polarities of an electrode pair. Hence the component of energy lost into the dielectric and in other forms of energy such as ultra-violet radiation, infra-red

radiation, visible light etc can be obtained.

3. The Expanding circle heat source model (ECHSM) model developed by Patel et al. [15] for the anode erosion can be studied with experimental results to investigate the influence of different machining parameters on the erosion rate.

4. Erosion rates of both the electrodes should be evaluated using Pointed heat source model (PHSM) and Expanding circle heat source model (ECHSM).

[8] S. Vaseekaran and C.A. Brown, "*Single discharge, spark erosion in TiB2 and Zinc Part I: Experimental*", Journal of Materials Processing Technology, Vol. 58, 1996, pp. 70-78.

[9] C.J. Heuvelman, H.J.A. Horsten, P.C. Veenstra, "*An Introductory Investigation of the Breakdown Mechanism in Electro-Discharge Machining*", Annals of CIRP, 1971

[10] F.S. Van Dijck and W.L. Dutre, "*Heat Conduction model for the claculation of the volume of molten metal in electric discharges*", J. Phys. D: Appl. Phys., Vol. 7,1974, pp. 898-910.

[11] S.M. Pandit and K.P. Rajurkar, "*Data Dependent Systems Approach to EDM process modeling from Surface Roughness profiles*", Annals of the CIRP, Vol. 29/1/1980, pp. 107-112.

[12] J.A. McGeough, H. Rasmussen, "*A macroscopic model of Electro Discharge machining*", International J. Mach. Tool Des. Res., Vol. 22, No. 4, 1982, pp. 333-339.

[13] P.C. Pandey and S.T. Jilani, "*Plasma channel growth and the resolidified layer in EDM*", Precision Engineering, April 1986, Vol. 8, No. 2, pp 104-109

[14] Daryl D.DiBitonto, Philip T.Eubank, Mukund R.Patel and Maria A.Barrufet, "*Theoretical models of the Electrical Discharge machining process - I. A simple Cathode Erosion model*", J. Appl. Phys., 66(9), 1 Nov., 1989, pp. 4095-4103.

[15] Mukund R.Patel, Maria A.Barrufet, Philip T.Eubank and Daryl D.DiBitonto, "*Theoretical models of the Electrical Discharge machining process - II. The Anode Erosion model*", J. Appl. Phys., 66(9), 1 Nov., 1989, pp. 4104-4111.

[16] Philip T.Eubank, Mukund R.Patel, Maria A.Barrufet and Bedri Bozkurt, "*Theoretical models of the Electrical Discharge machining process - III. The Variable Mass, Cylindrical Plasma model*", J. Appl. Phys., 73(11), 1 June, 1993, pp. 7900-7909.

[17] R. Snoeys, H. Cornelissen, K.U. Leuven, "*Correlation between Electro Discharge machining data and machining settings*", Annals of the CIRP, Vol. 24/1/1975, pp. 83-88.

[18] J. Longfellow, J.D. Wood and R.B. Palme, "*The effects of Electrode material properties on the wear ratio in Spark-Machining*", Journal of the Institute of metals, Vol. 96,1968, pp. 43-48.

[19] Kazimiez Albinski, "*The polarity of electrodes in Electro Discharge machining*", Proceedings International symposium for Electro machining - X1, pp. 95-103.

[20] Heng X1A, Masanori Kunieda, "*Research on machining characteristics of polarity changed pulse in EDM* ", Proceedings International Symposium for Electro machining -X1, pp. 181-190.

[21] B.R. Lazarenko, "The present state of development of Electrospark machining of conductive materials abroad", Electrospark Machining of Metals, Vol.2, edited by B.R. Lazarenko, (Consultants Bureau, Newyork, 1964), pp. 181-195

[22] V. George, V.C. Venkatesh, "*Investigation on Optimum machining conditions for Electo-Discharge machining of 5Cr Die steel*", Proceedings of the 9th AIMTDR Conference IIT-Kanpur, Dec. 1980, pp. 327-332.

[23] A. Erden, Faruk Arinc and Murat Kogmen, "*Comparison of Mathematical models for Electric Discharge Machining*", Journal of Materials Processing & Manufacturing Science, Vol. 4,Oct. 1995, pp. 163-176.

[24] P.C. Pandey and H.S. Shan, Modern Machining Process, Tata McGraw-Hill, NewDelhi, pp.97

Appendix A

CLAIBRATION CHART FOR R-35 GENERATOR

$t_{on} \rightarrow$	2000	1000	500	200	150	100	50	20	10	5	2	1
τ (Duty cycle) ↓ Position												
1	2600	2600	1500	600	440	260	230	117	73	45	27	14
2	2600	1940	1000	390	345	194	135	71	49	37	23	13
3	2600	1500	750	300	245	150	101	51	40	31	19	12
4	2350	1160	600	233	175	117	79	41	32	26	17	11
5	1850	920	460	180	140	92	66	34	27	23	15	10
6	1450	720	360	140	120	72	51	27	21	19	12	9
7	1125	565	280	110	90	56	41	21	17	16	11	9
8	860	440	214	90	70	43	31	16	13	12	9	7
9	640	320	160	60	60	32	22	12	10	10	7	6
10	440	220	110	40	40	22	16	8	7	7	5	5
11	270	130	70	30	32	14	10	5	5	5	3	3
12	130	60	30	10	10	6	5	3	2	2	2	2

The values against τ position is the pulse off-time for the corresponding pulse on-time.